

UNIVERSIDADE DE SÃO PAULO
INSTITUTO DE QUÍMICA

Programa de Pós-Graduação em Ciências Biológicas (Bioquímica)

MARIA ELISA ALMEIDA GÓES

Dissertação de Mestrado

**Kinin B2-Receptor in human iPSC differentiation
into cardiomyocytes**

Versão original da dissertação defendida

São Paulo

Data do Depósito na SPG: 06/08/2018

MARIA ELISA ALMEIDA GÓES

**Kinin B2-Receptor in human iPSC differentiation
into cardiomyocytes**

*Dissertação apresentada ao Instituto de
Química da Universidade de São Paulo para
obtenção do Título de Mestre em Ciências
Biológicas (Bioquímica)*

Orientador: Prof. Dr. Alexander Henning Ulrich

São Paulo

06/08/2018

Agradecimentos

Gostaria de agradecer, em primeiro lugar, a meus pais Glória Góes e Carlos Góes e minha irmã, Maria Clara Góes, por todo o apoio nesta trajetória e investimento em minha educação. Muito obrigada por sempre facilitarem minha tomada de decisões e por todo o amor que me doam diariamente.

Agradeço ao Prof. Dr. Henning Ulrich pela oportunidade de realizar o mestrado em seu laboratório, pelo apoio, confiança, orientação e por toda infraestrutura fornecida.

Ressalto minha gratidão ao Dr. Diogo Biagi, com quem aprendi o poder de uma sólida colaboração. Obrigada pelas dinâmicas trocas de ideias, por toda confiança depositada em mim e por todo suporte que nunca me negou. Agradeço a Jéssica Gonçalves e Rosanna Cerioni pelo trabalho na cultura celular, e a todos os membros da PluriCell Biotech (Dr. Diogo Biagi, Jéssica Gonçalves, Rosanna Cerioni, Dra. Estela Cruvinel, Dr. Marcos Valadares e Renato Leite), não só pela bem-sucedida colaboração, mas também pelo carinho com o qual sempre me receberam.

Deixo especiais agradecimentos ao Prof. Dr. Antônio Cassola, Dr. Carlos Basseto Jr., Dr. Arquimedes Cheffer e Dra. Ana Teresa Semeano que tantas vezes dedicaram tempo e energia para me ajudar a otimizar o uso do equipamento de eletrofisiologia. É difícil expressar em tão poucas palavras tudo o que vocês fizeram por mim.

Agradeço a minha madrinha científica, Dra. Juliana Corrêa-Velloso, por me guiar com tanto carinho durante cada uma de minhas questões pessoais e profissionais, por me ensinar a técnica de PCR em tempo real e sempre emprestar um pouco de toda sua experiência e maturidade para me ajudar a resolver meus problemas. Obrigada novamente, Juliana e Arquimedes, por corrigirem as primeiras versões de minha dissertação.

Também deixo um especial agradecimento a Erika Molina, aquela que em primeiro lugar me recebeu de braços abertos ao laboratório, e me ensinou muito mais do que as primeiras técnicas laboratoriais. Não esquecerei o seu incentivo a minha independência, apoio às minhas decisões, e reconhecimento dos meus pontos fortes, sem nunca deixar de me guiar naquilo que deveria ser melhorado.

Agradeço a Dra. Laura Sardá, por sempre me desejar força nos momentos de ansiedade que compartilhamos, pela confiança em colaborar comigo, e por realizar os experimentos de Western Blot deste trabalho. Obrigada Dra. Talita Glaser e Dra. Isis Nascimento por me ensinarem a técnica de imageamento de cálcio.

Obrigada Ana Paula Santos, Juliana Corrêa-Velloso, Ágatha Oliveira, Ana Teresa Semeano, Erika Molina, Maria Carolina Bittencourt, Yahaira Naaldijk, Arquimedes Cheffer e Laura Sardá por serem meus ombros amigos em todos os momentos de dificuldades e grandes parceiros nos momentos de alegrias – os últimos anos não teriam sido os mesmos sem vocês.

Também não posso deixar de mencionar aqueles que, embora ausentes no dia-a-dia, sempre fizeram questão de apoiar os meus passos e me ofertar carinho. À querida Lygia Aguiar (aquele que chamo de meu diário ambulante), foi ótimo compartilhar contigo tantos momentos e sorvetes ao longo dos últimos oito anos. Aos biólogos felpudos, aos amigos do ensino médio e aos amigos de intercâmbios, agradeço as múltiplas conversas motivadoras, por sempre se preocuparem tanto comigo e por tantos momentos divertidos. Realmente me considero uma pessoa privilegiada por ter tantas pessoas maravilhosas perto de mim.

Por fim, agradeço ao Professor Dr. João B. Pesquero pela doação da droga Firazyr, ao Conselho Nacional de Desenvolvimento Científico e Tecnológico (CNPq) pela bolsa e verba concedida ao projeto, e a Fundação de Amparo à Pesquisa do Estado de São Paulo (FAPESP) pela verba concedida ao laboratório.

*Nothing in life is to be feared,
it is only to be understood.
Now is the time to understand more,
so that we may fear less.*
— Marie Curie

Any intelligent fool can make things bigger and more complex...

*It takes a touch of genius
— and a lot of courage —
to move in the opposite direction.*

— Albert Einstein

RESUMO

Góes, M.E.A. Receptor B2 de cininas na diferenciação de iPSC humanas em cardiomiócitos 2018. (91P). Dissertação de Mestrado - Programa de Pós-Graduação em Ciência Biológicas (Bioquímica). Instituto de Química, Universidade de São Paulo, São Paulo.

Doenças cardiovasculares são responsáveis por quase um terço de todas as mortes globais anualmente, e por isto o sistema cardiovascular é amplamente estudado. Cardiomiócitos derivados a partir de células-tronco pluripotentes induzidas humanas (hiPSC-CM) emergiram como uma promissora tecnologia para modelagem de doenças cardíacas e terapia personalizada. No entanto, desafios acerca de sua maturação funcional e molecular ainda são enfrentados. Além disso, protocolos de diferenciação geralmente levam à obtenção de populações heterogêneas contendo células com fenótipos similares aos de cardiomiócitos nodais, atriais e ventriculares sendo, portanto, inapropriadas para fins terapêuticos. A bradicinina (BK) é um peptídeo vasoativo que exerce importantes papéis fisiológicos no sistema cardiovascular, além de ter sido previamente descrita como importante para a diferenciação neuronal, de queratinócitos e de músculo esquelético. Este projeto foi realizado em colaboração com a empresa PluriCell Biotech, uma startup especializada na produção e diferenciação de hiPSC-CM, e buscou (1) caracterizar a expressão gênica e proteica de marcadores moleculares de maturação e de especificação de subtipos cardíacos durante a diferenciação; (2) avaliar a funcionalidade elétrica de hiPSC-CM por meio da caracterização de seus potenciais de ação (PAs) e (3) Investigar se o progresso da diferenciação de hiPSC-CM é regulado por bradicinina por meio do receptor B2 (B2R). Nossos resultados validaram o modelo que propõe um *switch* na expressão das isoformas funcionais de troponina I esquelética (ssTnI) e cardíaca (cTnI), durante o desenvolvimento e diferenciação celular, pelo menos parcialmente. Além disso, tempo prolongado em cultura resultou em maiores níveis de expressão do marcador ventricular MLC2v, assim como maiores frequências de PAs com morfologias similares a de cardiomiócitos ventriculares. Análise eletrofisiológica de hiPSC-CM revelam a existência de uma população mista contendo PAs correspondentes aos subtipos nodais, atriais e ventriculares, assim como pronunciada automaticidade e outros atributos típicos de cardiomiócitos imaturos, como baixa amplitude e devagar velocidade de despolarização. Estes resultados são coerentes com os de outros grupos que ainda não foram totalmente bem-sucedidos em diferenciar células cardíacas maduras similares a

cardiomiócitos nativos a partir de células-troncos pluripotentes. Após mostrar que as hiPSC-CM expressam receptores B2 funcionais e responsivos, submetemos o receptor a uma ativação crônica com BK 10 μ M e BK 1 μ M ou inibição crônica com Firazyr 5 μ M + BK. Apesar da modulação do B2R não ter interferido de forma negativa no rendimento da diferenciação ou na morfologia celular, análise de expressão gênica e proteica de ssTnI e cTnI e do marcador ventricular MLC2v não revelou resultados significativos em comparação aos controles não-tratados. Isto sugere que a BK não interfere na maturação e especificação de subtipos cardíacos em hiPSC-CM, apesar de não podermos ignorar o fato de que ela poderia estar desencadeando outros efeitos inexplorados. Nós recomendamos um estudo mais aprofundado acerca de quais vias de sinalização se tornam ativas após estimulação do receptor B2 em hiPSC-CM, com o objetivo de afunilar quais processos celulares poderiam ser investigados em uma próxima etapa deste estudo.

Palavras-chave: hiPSC, cardiomiócitos, maturação, bradicinina, receptor B2, eletrofisiologia

ABSTRACT

Góes, M.E.A. **Kinin B2-Receptor in human iPSC differentiation into cardiomyocytes.**

(91P). Masters Thesis – Graduate Program in Biochemistry. Instituto de Química, Universidade de São Paulo, São Paulo.

Cardiovascular diseases are responsible for almost one third of all global deaths yearly, and therefore are largely studied. Cardiomyocytes derived from human induced pluripotent stem cells (hiPSC-CM) have emerged as an exciting technology for cardiac disease modelling and personalised therapy. Nevertheless, issues concerning functional and molecular maturation are still faced. In addition to this, differentiation protocols generally yield a heterogeneous mixed population comprised of nodal, atrial and ventricular-like subtypes, being unsuitable for therapeutic purposes. Bradykinin (BK) is a vasoactive peptide which exerts important physiological roles in the cardiovascular system, having been previously described as important for cellular, keratinocyte and skeletal muscle differentiation. This project performed in cooperation with PluriCell Biotech, a startup specialized in the production and differentiation of hiPSC-CM, has sought (1) characterizing gene and protein expression of molecular markers of maturation and of subtype specification throughout of differentiation; (2) Assessing the electrical functionality of hiPSC-CM through the characterization of subtype-specific action potentials (APs) and (3) Investigating whether the progress of hiPSC-CM maturation is regulated by BK through kinin-B2 receptors (B2R). Our results have validated the model that proposes a developmental-dependent switch between skeletal (ssTnI) and cardiac (cTnI) isoforms of troponin I as differentiation progresses, at least to some extent. Furthermore, prolonged time in culture has resulted in higher levels of expression of the ventricular marker MLC2v and in increased rates of ventricular-like action APs. Electrophysiological analysis of hiPSC-CM reveals a mixed population with AP morphologies correspondent to nodal, atrial and ventricular subtypes, all showing pronounced automaticity as well as other features of immature cardiomyocytes, such as low amplitude and depolarization velocity. Such findings are coherent with those from other groups who have attempted to differentiate mature native-like cardiac cells from pluripotent stem cells sources, without fully succeeding. After showing that differentiating hiPSC-CM express a functional and responsive B2R, the receptor was subjected to chronic activation with 10 μ M BK and 1 μ M BK or inhibition with 5 μ M Firdazir+BK. Even though B2R modulation has not interfered negatively with differentiation yields nor cell morphology, analysis of gene and

protein expression of ssTnI or cTnI and of the ventricular marker MLC2v, have revealed no significant results in comparison to untreated controls. This suggests that BK does not interfere on hiPSC-CM maturation nor subtype specification, although we cannot rule out that it could be leading to other unexplored effects. We recommend a closer look into which intracellular signalling pathways become active upon B2R stimulation in hiPSC-CM, in order to narrow down cellular processes for further investigation.

Keywords: hiPSC, cardiomyocytes, maturation, bradykinin, kinin B2 receptor, electrophysiology

LIST OF FIGURES

Figure 1. Phases and kinetics of a ventricular cardiomyocyte..	18
Figure 2. Schematic representation of the kinin-kallikrein system..	29
Figure 3. Schematic representation of signalling cascade triggered in response to B2R activation by bradykinin (BK)..	30
Figure 4. Timeline of hiPSC differentiation, experimental and drug treatment timepoints.	39
Figure 5. Relative expression of <i>TNNI1</i> and <i>TNNI3</i> genes by RT-qPCR throughout cardiac <i>in vitro</i> differentiation.	50
Figure 6. Co-expression of ssTnI and cTnI or MLC2v and ACTN2 in different timepoints of hiPSC differentiation by flow cytometry..	52
Figure 7. Representative subtype-specific AP traces in the hiPSC-CM population.	54
Figure 8. Distribution of cardiac subtypes in a hiPSC-CM population.	55
Figure 9. AP kinetic parameters from hiPSC nodal, atrial and ventricular subtypes in time intervals between the 33 rd and 48 th day of differentiation.	57
Figure 10. Analysis of B2R expression and activity in hiPSC on the 5 th day of differentiation.	58
Figure 11. Relative <i>TNNI1</i> and <i>TNNI3</i> gene expression of hiPSC-CM differentiated in the presence of 10µM BK or subjected to B2R inactivation with 5µM Firazyr followed by stimulation with 10µM BK, in relation to control.	60
Figure 12. ssTnI/cTnI and MLC2v protein expression in hiPSC-CM differentiated in the presence of 10µM BK or subjected to B2R inactivation with 5µM Firazyr followed by stimulation with 10µM BK, on day 15 of differentiation.	61
Figure 13. Effect of B2R activation or inhibition on the efficiency of cardiac differentiation from hiPSC.	63
Figure 14. Gene and protein expression of troponin I isoforms and MLC2v following pharmacological activation of B2R with 1µM BK or blockade with 5µM Firazyr during cardiac <i>in vitro</i> differentiation from hiPSC.	64

LIST OF TABLES

Table I: Primer sequences for each gene analysed, respective primer size and amplicon size.....	41
Table II: List of antibodies employed in western blot experiments.....	45
Table III: List of antibodies employed in flow cytometry experiments.....	46

LIST OF ABBREVIATIONS

ACE – Angiotensin converting enzyme

ANOVA – Analysis of Variance

AP – Action Potential

APD₅₀ – Action potential duration at 50% of repolarization

APD₉₀ - Action potential duration at 90% of repolarization

B1R – B1 receptor

B2R – B2 receptor

BK - Bradykinin

cTnI – Cardiac troponin I

DAG – Diacylglycerol

dV/dT_{max} – Maximum rate of depolarization

HCN4 - Hyperpolarization Activated Cyclic Nucleotide Gated Potassium Channel 4

hESC – Human embryonic stem cells

hiPSC– Human induced pluripotent stem cells

HMWK – High molecular weight kininogens

hPSC– Human pluripotent stem cells

I_{Ca} - Inward Ca²⁺ current

I_f– Funny current

I_{K1} – Inward rectifier current

I_{Kr} - Rapid delayed rectifying currents

I_{Ks} - Slow delayed rectifying currents

IP3 – Inositol triphosphate

I_{To} -Transient outward current

KCNJ2 - (Potassium Voltage-Gated Channel Subfamily J Member 2)

KCNQ1 - Potassium Voltage-Gated Channel Subfamily Q Member 1

KD - Kallidin

KKS – Kinin-kallikrein system

LMWK – Low molecular weight kininogens

MAPK – Mitogen Activated Phosphate Kinases

MHC – Myosin heavy chain

MLC2a - Myosin regulatory light chain 2, atrial isoform

MLC2v - Myosin regulatory light chain 2, ventricular isoform

NEP – Neutral endopeptidase

PCR – Conventional polymerase chain reaction

PIP2 - Phosphatidylinositol 4,5-bisphosphate

PKC – Protein Kinase C

PLC – Phospholipase C

PSC– Pluripotent stem cells

RMP – Resting Membrane Potential

RT-qPCR – Semi-quantitative reverse transcription real-time polymerase chain reaction

RyR2 – Ryanodine receptor 2

SERCA ATPase - Sarcoendoplasmic reticulum calcium transport ATPase

SLN - Sarcolipin

SR – Sarcoplasmic Reticulum

ssTnI – Slow skeletal troponin I

TnC – Troponin C

TnI– Troponin I

TNNI1 - TnI-skeletal-slow-twitch

TNNI2 - TnI-skeletal-fast-twitch

TNNI3 - TnI-cardiac

TnT– Troponin T

TABLE OF CONTENTS

1. INTRODUCTION.....	17
1.1. Cardiovascular diseases, <i>in vivo</i> models and the cardiac action potential.....	17
1.2. <i>In vitro</i> models for CVDs studies.....	19
1.3. Cardiac <i>in vitro</i> differentiation.....	21
1.3.1. hiPSC-CM maturation status.....	24
1.4. The kinin-kallikrein system and the cardiovascular system.....	27
2. JUSTIFICATIVE	34
3. OBJECTIVES	36
3.1. Specific Objectives.....	36
4. MATERIALS AND METHODS	38
4.1. iPSC generation, differentiation and culturing.....	38
4.2. RNA extraction and cDNA conversion.....	40
4.3. Conventional polymerase chain reaction (PCR)	40
4.4. Semi-quantitative reverse transcription real time PCR (RT-qPCR).....	41
4.5. Saline Solutions.....	42
4.5.1. Patch clamp saline solutions	42
4.5.2. Ca^{2+} imaging.....	42
4.6. Whole-cell patch-clamp	43
4.7. Measurement of changes in free intracellular Ca^{2+} ($[\text{Ca}^{2+}]_i$) concentration	43
4.8. Protein isolation and Western Blot.....	44
4.9. Flow cytometry	45
5. STATISTICAL ANALYSIS.....	48
6. RESULTS	50
6.1. Characterization of <i>TNNI1</i> and <i>TNNI3</i> expression throughout hiPSC-CM differentiation. 50	
6.2. Characterization of ssTnI, cTnI, ACTN2 and MLC2v protein expression throughout hiPSC-CM differentiation.	51
6.3. Characterization of the action potential of hiPSC-CM.....	53
6.3.1. Classification of the proportions of atrial, ventricular and nodal subtypes	53
6.3.2. Analysis of time-dependent changes in the AP kinetics	56
6.4. Expression of B2R in differentiating hiPSC-CM, and verification of its responsivity to BK 58	
6.5. Evaluation of hiPSC-CM phenotypes following B2R activation or inhibition during differentiation.	59

6.5.1.	<i>TNNI1</i> and <i>TNNI3</i> expression following B2R activation with 10μM BK or inhibition with Firazyr	59
6.5.2.	Expression of cTnI, ssTnI, MLC2v in hiPSC-CM following B2R activation with 10μM BK or inhibition with 5μM Firazyr	61
6.5.3.	Gene and protein expression of troponin I isoforms and MLC2v following B2R activation with 1μM BK or inhibition with 5μM Firazyr	62
7.	DISCUSSION	67
7.1.	Characterization of Troponin I gene and protein expression throughout hiPSC-CM differentiation.	67
7.2.	Characterization of the electrophysiology of hiPSC-CM.....	69
7.2.1.	Analysis of the proportions of atrial, ventricular and nodal subtypes	69
7.2.2	Analysis of time-dependent variations in AP kinetics	70
7.3	Effect of modulation of B2R on the molecular maturation of hiPSC-CM.....	73
8.	CONCLUSIONS.....	79
9.	BIBLIOGRAPHIC REFERENCES	81
10.	ANEXOS.....	90
A –	SÚMULA CURRICULAR	90

INTRODUCTION

1. INTRODUCTION

1.1. Cardiovascular diseases, *in vivo* models and the cardiac action potential

Cardiovascular diseases (CVDs) are, according to the World Health Organization, the most frequent cause of death globally, representing almost one third of all deaths. CVDs comprise a group of heart and blood vessels' disorders, including congenital diseases, but are also related to chronic diseases, nutrition, environmental stressors and lifestyle (1). For these reasons, lots of effort and investment is put on the study of CVD physiology, prevention, surgery, therapy and drug development.

Animal models are often employed in the study of the pathophysiology of CVDs. Myocardium infarction, heart fibrillation, hypertrophy and failure can be modelled in small animals subjected to surgical interventions (2). In addition to this, genetically engineered mice are frequently employed in arrhythmia studies (2,3). Further, animals have repeatedly been recipients of cell grafts in studies that seek optimizing the technology of cell therapy (4–7). Still, despite their historical contribution for drug development and for the understanding of the heart physiology, one must be careful when extrapolating data from small animal studies to better understand the physiology of the human heart (2). This is due to important interspecific differences in the electrophysiological properties of heart cells (8).

The heart is composed of different cellular types, comprising not only contractile cells (cardiomyocytes) but also noncontractile cells, such as cardiac fibroblasts, endothelial cells and perivascular cells (9). Structurally, the mammalian heart can be subdivided into four independent chambers, two atriums and two ventricles, which contain, respectively, atrial and ventricular cardiomyocytes (among other cell types). Another relevant cardiomyocyte subtype that can be found in the myocardium are pacemaker cells – a cluster of cells located on the

right atrium, which generates electrical impulses - action potentials - and therefore “dictate” the contraction rhythm of the heart (10).

Cardiomyocytes are highly specialized cells which are physically and electrically coupled to each other, responding to rhythmic stimuli (11). One of the most prominent phenotypic characteristics of cardiomyocytes is their electrical activity and consequent generation of action potentials (APs). The cardiac AP is tightly regulated by at least six ionic currents coordinated in time, as shown in Fig.1. APs are triggered by an electric excitatory stimulus and initiated by a rapid upstroke depolarization phase (phase 0), due to the brief opening of Na^+ channels and Na^+ influx. Ca^{2+} channels open in sequence, and the inward Ca^{2+} current (I_{Ca}) is responsible for the plateau observed in phase 2 of the ventricular AP, also triggering myocardium contraction. Finally, four major K^+ currents contribute to cardiac repolarization during phases 3 and 4: the K^+ transient outward current (I_{To}) causes the notch observed in phase 1; I_{Ks} and I_{Kr} bring the membrane potential back to resting membrane potential of -90mV in phase 3 and are called, respectively, slow and rapid delayed rectifying currents. Finally, I_{K1} (inward rectifier current) maintains the resting state in phase 4 (2,11).

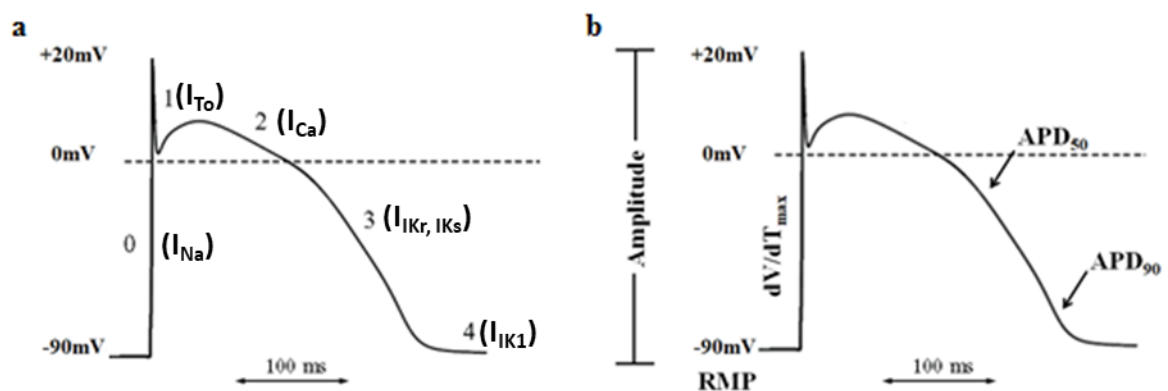


Figure 1. Phases and kinetics of a ventricular cardiomyocyte. a) Numbers indicate the phases of the action potentials, while the major ionic currents for each phase are represented in grey. b) Kinetic parameters that describe a cardiac action potential. RMP: Resting Membrane Potential; dV/dT_{max} : maximum rate of depolarization; APD_{50} : Action potential

duration at 50% of repolarization and APD₉₀: Action potential duration at 90% of repolarization. Modified from Sigg *et al*, 2010 (2).

The complexity of cardiomyocyte AP underlies many physiological aspects of the healthy heart, as well as of pathological conditions, once mutations in genes that encode for ion channels can result in arrhythmias (12,13). According to Sinnecker (8), not only are action potentials shapes and frequencies different from species to species, but also the repolarization phase of the AP will be governed by different ion currents depending on the model studied, which makes them unsuitable for the accurate modelling of cardiac diseases (12,14–17).

For instance, the most relevant repolarizing currents in the human heart are delayed rectifier I_{kr} and I_{ks} . Meanwhile, the I_{to} as well as currents not displayed in human ventricles are quite relevant for the repolarization of mouse ventricular cardiomyocytes (2,15). Consequently, some clinically relevant cardiac phenotypes caused by genetic syndromes cannot be accurately modelled in mice. This is the case of long-QT syndrome type 1, a familial arrhythmogenic syndrome initiated by a mutation in the Potassium Voltage-Gated Channel Subfamily Q Member 1 gene (*KCNQ1*), which encodes for a mutant hERG K^+ ion channel, leading to abnormal channel function and delayed cell repolarization, ultimately causing death (16,17). Still, the phenotype observed in humans is not faithfully reproduced in *Kcnq1* knockout mice (12,14), raising the need of the development of more appropriate alternatives for modelling genetic cardiac diseases.

1.2. *In vitro* models for CVDs studies

Human adult cardiomyocytes are the ideal *in vitro* model to study CVDs, but have a remarkably limited source, being mostly derived from either biopsies of elderly patients with already remodelled organs, or from hearts of patients who suffered brain death. Besides, the isolation process itself is rather challenging due to the strong connections between cells and

the extracellular matrix (2,18). In addition to this, adult cardiomyocytes are mostly postmitotic nondividing cells, being thus unsuitable for long-term *in vitro* experiments, not to mention large scale studies (2). Nevertheless, no immortalized cell line which consistently mimics APs and other important features of native cardiomyocytes has so far been established (8).

In 1998, Thomson *et al.* (19) derived the first human embryonic pluripotent stem cells (hESC) from human blastocysts. hESC are able to differentiate into tissues derived from the three germ layers, thus having a potential to generate any tissue of the human body. The number of works exploring hESC rose exponentially in the subsequent years, including hESC differentiation into cardiomyocytes (20–22). However, hESC research raised not only abundant volume of data, but also ethical concerns, due to the use of human embryos in the process.

The need of seeking alternatives to hESC led Takahashi and Yamanaka (23) to develop the so-called induced pluripotent stem cells (iPSC) using a method that involved the retroviral delivery of four specific transcription factors (Oct3/4, Sox2, c-Myc, Klf4) to fibroblasts, resulting in genetic reprogramming towards an embryonic-like state. The reprogrammed cells presented, then, the ability to be further differentiated into a variety of tissues of all three germ layers. iPSC are therefore a potent technology with promising application for diverse fields of cell biology, among them, CVDs (8).

In fact, human iPSC-derived cardiomyocytes (hiPSC-CM) have been demonstrated as phenotypically and functionally equivalent to hESC-CM (24) and have, therefore, been explored regarding their multiple applications: first, hiPSC-CM constitute a potentially unlimited source of cardiomyocytes for downstream applications, such as screening of drugs that can be beneficial for CVDs (25). Second, they can be employed for cardiotoxicity

screening in the pharmaceutical industry, reducing unnecessary use of animals while augmenting the specificity of the employed model (26). Third, the possibility of deriving cardiomyocytes from patients with varied genetically-caused diseases goes along with the worldwide tendency of developing personalised therapy. This is important because although some cardiac genetic diseases display similar clinical manifestations, slight variations in their phenotypes can be observed and account for the diagnostics and outcomes of the treatments (13,27). Ultimately, the use of hiPSC-CM in autologous cell therapy would avoid the need of concomitant immunosuppression (6).

1.3. Cardiac *in vitro* differentiation

In order to obtain high quality cardiomyocytes it is fundamental to comprehend the process of cardiac differentiation, which has so far been perceived as complex and tightly regulated by epigenetic factors, extracellular signals and diverse molecular pathways (28,29). *In vitro* differentiation methods have advanced considerably in the last decade, over which a series of protocols have been derived and progressively improved regarding purity and yield (30). In general, differentiation protocols seek mimicking the key *in vivo* developmental stages that occur during cardiogenesis, by inducing the differentiation of the original pluripotent stem cell (PSC) population into an intermediary mesodermal stage, and then further introducing biochemical signals that lead these cells to commit with a cardiomyogenic fate (31).

Nevertheless, most available protocols still generate a heterogeneous mix of cardiomyocytes containing at least three cardiomyocytes subtypes: ventricular-like, atrial-like and nodal-like cardiomyocytes, with specific AP properties (32). However, in order to fully make use of hiPSC-CM potential in regenerative medicine, it is imperative that homogeneous populations of each cardiomyocyte subtype can be generated, thus avoiding the

arrhythmogenic potential of performing cell therapy with a mixed cardiomyocyte population (32).

Some molecular markers have been proposed as appropriate indicators of cardiomyocyte subtypes. This is the case of Iroquois homeobox 4 (*Irx-4*), a ventricular-specific transcription regulator which has been proposed as a possible driver of ventricle development (33). The sarcomeric myosin light chain proteins MLC2v (encoded by the gene *MYL2*) and MLC2a (*MYL7*) are, respectively, commonly used markers to discriminate ventricular and atrial cells from mixed populations. In fact, although MLC2v is exclusively expressed in the ventricle, since the onset of cardiomyogenesis, MLC2a is initially expressed as a pan-cardiac gene (34). Then, as heart development progresses, MLC2a expression becomes restricted to the atrial chambers (33).

Sarcolipin (*SLN*) is an atrium-specific Ca^{2+} -binding protein being expressed at the embryonic day E.11.5 of mouse development (33). A proof-of-concept study was successful in demonstrating that hiPSC-CM express sarcolipin and sorted differentiating cardiomyocytes that expressed a fluorescent *SLN* gene construct, further showing that these cells displayed a molecular and functional atrial phenotype (35).

The definition of an appropriate marker for the discrimination of nodal cells is still under debate. *HCN4* (Hyperpolarization Activated Cyclic Nucleotide Gated Potassium Channel 4) is a protein coding gene that encodes for a membrane channel which opens on hyperpolarized cell membrane states (10). This channel generates the pacemaker current, also known as I_f or funny current, and whose activity is responsible for the spontaneous contractility of the heart (10,36). While in the native heart, the expression of *HCN4* is restricted to nodal cells (37), immature cardiomyocytes derived from pluripotent stem cell

sources (PSC-CM) have been shown to persistently express *HCN4* and spontaneous beating (35) (see section 1.3.1), limiting its usefulness as a nodal marker.

Because specific and stable subtype markers are still being sought, the gold standard for the classification of cardiomyocytes is still the electrophysiological analysis of single cell APs (38,39). This is possible due to the fact that each cardiomyocyte subtype displays different AP kinetic parameters (Fig. 1b) (37). Human ventricular myocytes are known to display a resting membrane potential (RMP) of approximately -90mV and an amplitude of more than 100mV (2). The maximum rate of depolarization (dV/dT_{\max}) of the human ventricle is extremely fast and can reach 300V/s (37,40,41). Because of the characteristic I_{Ca} existing in the phase 2 of the ventricular AP, it is possible to remark a long plateau existing after depolarization. Consequently, the ventricular action potential duration at 50 and 90% of repolarization (APD_{50} and APD_{90}) is also larger, with reports ranging from 270ms to 550ms (42). Atrial myocytes, on the other hand, have an intermediate RMP, which usually varies between -60mV and -80mV, a dV/dT_{\max} of 200V/s and a less pronounced I_{Ca} plateau (which consequently lowers APD_{90} to around 170ms) (37,43). Finally, nodal myocytes have a more depolarized RMP (-60mV) and APs of lower amplitude (80mV) and remarkably slower dV/dT_{\max} (approximately 5V/s) (37).

Recently, advances have been made towards orientating PSC differentiation towards each specific cardiac cell type. Inhibition of Wnt/ β -catenin signalling with a small synthetic molecule called IWR-1 has been suggested as a good strategy to induce a commitment with the ventricular phenotype (44). Weng and collaborators (45) developed a cost-effective protocol that yields more than 85% $MLC2v^+$ cells and more than 90% cardiomyocytes with a ventricular-like AP signature from five different pluripotent stem cell lines. Alternating retinoid signals following bone morphogenic protein inhibition with Noggin has also been reported to specify either atrial or ventricular fate: according to Zhang *et al.* (46), while

addition of retinoic acid to noggin-treated cells resulted in low *IRX-4*, low MLC2v expression and 94% of atrial-like APs, inhibition of retinoic acid signalling results in increased *IRX-4* and MLC2v expression, as well as 83% ventricular-like APs. Fewer studies have explored the orientation of PSC-CM into pacemaker cells, despite the potential usefulness of engineering a biological pacemaker (47–49). For instance, one relatively successful approach towards the generation of a predominantly nodal cardiomyocyte population include conditioning immature hiPSC-CM colonies with visceral endoderm-like factor, rendering myocytes that display regular spontaneous electrical activity and that are responsive to adrenergic/cholinergic stimulation (48).

1.3.1. hiPSC-CM maturation status

One of the greatest challenges that still hamper the use of hiPSC-CM in therapy regards their maturity. Cardiomyocytes derived from pluripotent stem cells present some features of fetal myocytes rather than showing a fully adult phenotype (50). This is observed concerning not only gene and protein expression, but also hiPSC-CM functionality (51).

Heart contraction is a highly organized process that involves the sliding of actin and myosin filaments, with expenditure of energy. The molecular mechanism of muscle contraction has been thoroughly studied and is reviewed in (52). Basically, this process is regulated by the heterotrimeric troponin complex, which is present in skeletal and cardiac muscles, consisting of three regulatory proteins filaments called troponin C, troponin T and troponin I (TnC, TnT and TnI, respectively). Altogether, they are responsible for controlling the Ca^{2+} -dependent interaction between actin and myosin filaments.

The TnI subfamily comprises three genes: TnI-skeletal-slow-twitch (*TNNI1*) TnI-skeletal-fast-twitch (*TNNI2*), and TnI-cardiac (*TNNI3*). The *in silico* analysis of each gene sequence shows that, phylogenetically, it is likely that a *TNNI2* ancestral gene was duplicated

and diverged, originating a *TNNI1*-like sequence, which would have gone through a second round of duplication and diverged into the current *TNNI1* and *TNNI3* genes (53). While *TNNI2* is only expressed in skeletal-fast-twitch muscle fibers, both *TNNI1* and *TNNI3* are expressed in the mammalian heart (54).

Physiologically, TnT positions tropomyosin molecules on the actin filament, preventing the interaction between myosin and actin; TnI binds to actin and to the troponin-tropomyosin complex, holding them in place. When Ca^{2+} ions are released, they bind to TnC causing a conformational change in the complex. The tropomyosin complex is withdrawn from the actin filament, uncovering the myosin-binding sites and triggering contraction (11).

The general mechanism for muscle contraction is quite similar on the cardiac and skeletal muscles, but some important differences can be noticed, such as the fact that the N-terminal extension of TnI-cardiac (cTnI) can be phosphorylated in multiple sites, resulting in myofibrils' desensitization to Ca^{2+} (55) among other physiological alterations (53). TnI-skeletal-slow-twitch (ssTnI), on the other hand, is not subjected to such regulatory mechanisms and shows higher cooperativity and affinity to Ca^{2+} , especially under acidic environments, making the muscle more resistant to hypoxic events that may occur during the gestational period (53,55,56). It seems, then, that the different TnI isoforms during cardiogenesis may have the role of fine tuning myofilament adaptation to the microenvironment and contractile performance (53).

One remarkable developmental feature of troponin I expression, is that, *in vivo*, ssTnI is only expressed in the fetal/neonatal heart. During heart development there is a switch in TnI proteic isoform expression: ssTnI expression is slowly reduced, while cTnI isoform is progressively more expressed, being the only isoform expressed in the adult heart (54,57). Previous studies have reported that PSC-derived cardiomyocytes express a mix of ssTnI and

cTnI proteins, having thus not yet reached a fully mature molecular phenotype. The ssTnI/cTnI conversion is proposed to occur in a 1:1 stoichiometric conversion which is not reversible following stress situations, such as ischemic heart diseases and heart failure. For these reasons, the expression troponin I isoforms can be used as markers of cardiac maturation status (53,57).

PSC-CM often display immature functional phenotypes regarding electrophysiology, Ca^{2+} homeostasis and contraction force (51). Their action potential shapes reveal a slower rise slope (dV/dt_{\max}), shorter duration, a more depolarized resting membrane potential and marked auto-excitation activity – in resemblance to embryonic hearts' (24). The Ca^{2+} homeostasis of PSC-CMs also reveals the existence of an immature sarcoplasmic reticulum (SR), an organelle which plays an important role in excitation-contraction coupling during each cardiac cycle. Briefly, a small Ca^{2+} influx through L-type Ca^{2+} channels activates ryanodine receptors (RyR2) located in transverse tubules, triggering a rapid release of great amounts of Ca^{2+} stored in the SR. This process is known as Ca^{2+} -induced Ca^{2+} release, and accounts for the plateau observed in the ventricular AP and the systolic contraction of myofibrils (58). During diastole, SR Ca^{2+} ATPase (SERCA) actively reuptakes cytoplasmic Ca^{2+} , allowing fibrils relaxation (59–61). It has been shown that iPSC-derived cardiomyocytes display an underdeveloped SR, with a smaller storage volume and poorer responsivity to RyR2 and SERCA ATPase pharmacological modulation (62). Finally, sarcomere contraction force of the most advanced engineered heart tissues display, still, only half the peak twitch tension of the native human myocardium ($44 \pm 11.7\text{mN/mm}^2$) (32,63).

Because PSC-CM immaturity still represents an unsolved issue towards the application potential of this technology, it is highly important that differentiation and maturation protocols are performed in a rational and controlled manner. Some of the attempted strategies to perfect these include enhancing time in culture (64–66) and mimicking

in vivo maturation (32), by employing biomaterials, chemical and electrical cues, co-culturing with other cell types, among others (28,30,66,67). In addition to this, modulation of biochemical signalling has also contributed towards a more mature phenotype in hiPSC-CM. The most commonly modulated pathways are molecules that induce IGF/Akt signaling (68), such as insulin growth factor, fibroblast growth factor and vascular endothelium growth factor (32). Furthermore, β -adrenergic stimulation has been reported to improve contractile function of the heart (32), and the triiodothyronine hormone can induce maturation of the SR in later phases of differentiation (51,62).

Although the knowledge regarding cardiomyocyte differentiation is being exponentially built up, modulation of *in vitro* cell differentiation has so far not accomplished state-of-art PSC-CM. There is, therefore, a vast field of research regarding molecules and biological pathways intricately involved in this process. In this way, this project proposed to study the process of cardiac differentiation and maturation by exploring the kinin-kallikrein system (KKS), a multienzymatic system which has been extensively described as important for heart physiology and disease (69–73). Moreover, the KKS has been implicated in cell differentiation of at least three other cell types: neurons, keratinocytes and skeletal muscle cells. (74–80).

1.4. The kinin-kallikrein system and the cardiovascular system

The KKS is a multienzymatic system and has been first described by Abelous and Bardier (81) as responsible for the lowering of blood pressure after intravenous urine injection. Kinins are generated from the breakdown of high and low molecular weight (HMW and LMW, respectively) kininogens by serine proteases called kallikreins (82), releasing the oligopeptides bradykinin (BK) and kallidin (Lys-BK or KD) (Fig.2). Typically, HMW-kininogens circulate in the plasma and give rise to BK, which is composed of 9 amino acids

residues (Arg-Pro-Pro-Gly-Phe-Ser-Pro-Phe-Arg) and participates in the regulation of blood coagulation, inflammation and blood pressure control (70,83,84). LMW-kininogens, for instance, can be found in the tissues and their cleavage continuously releases kallidin (Lys-Arg-Pro-Pro-Gly-Phe-Ser-Pro-Phe-Arg), believed to have a physiological regulatory role (72).

Kinins are, in general, short-lived peptides with an *in vivo* half-life of 30 seconds (85), being subsequently degraded by kininases, rendering inactive peptides of 7 or 5 amino acids. The most relevant kininase involved in kinins degradation are kininase II, or angiotensin converting enzyme (ACE) and the neutral endopeptidase (NEP).

Cleavage of BK and KD by kininase I (carboxypeptidase M/N) leads to loss of C-terminal arginine residue, resulting in the formation of desArg⁹-BK and desArg¹⁰-KD, which stimulate B1 receptors. B1 receptors (B1R) are not constitutively expressed, being normally expressed prior to the induction of an inflammatory response to bacterial endotoxins or cytokines (72).

Both bradykinin and kallidin mediate their effects through B2 receptors (B2R), which are constitutively expressed in various tissues, among them the cardiovascular system, including blood vessels (86) and heart cells (87). B1R and B2R are metabotropic transmembrane G-protein-coupled receptors (84).

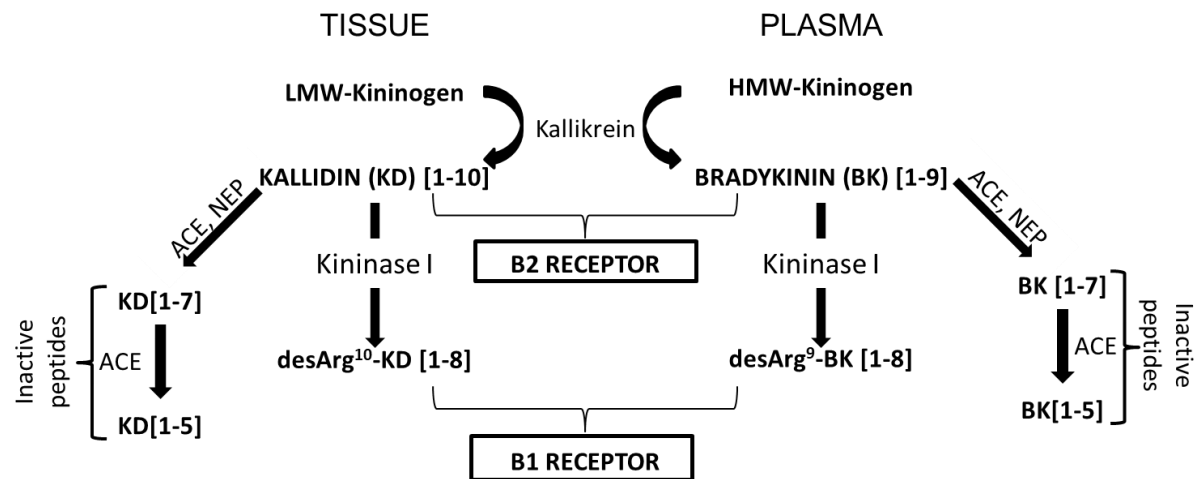


Figure 2. Schematic representation of the kinin-kallikrein system. Kinin B2 receptor is stimulated by BK and KD, which result from the kallikrein-mediated breakdown of LMW and HMW. Further enzymatic degradation of KD and BK by kininase I result in the removal of C-terminal arginine residue, rendering desArg¹⁰-KD and desArg⁹-BK, agonists of the Kinin B1 receptor. Degradation by ACE results in shorter inactive peptides.

Activation of Gq-coupled receptors by kinins triggers phospholipase C (PLC)-catalysed hydrolysis of PIP₂ (phosphatidylinositol 4,5-bisphosphate), a minor phospholipid component of cellular membranes, into inositol triphosphate (IP₃) and diacylglycerol (DAG), as represented in Fig.3 (88). IP₃ acts on IP₃-receptors on the sarcoplasmic reticulum, triggering the release of Ca²⁺ ions, which, on their turn, act as second messengers on downstream signalling cascades (89–91). DAG, on the other hand, is an allosteric activator of protein kinase C (PKC), which elicits numerous biological effects, such as inflammation, cellular proliferation, differentiation, transformation and cell death (92).

For instance, PKC has been shown to control cellular proliferation, upon inducing phosphorylation-dependent internalization of epidermal growth factor receptors (93) and of the proto-oncogene receptor tyrosine kinase HER-2 (88). In addition to this, PKC is also involved in regulation of the mitogen-activated protein kinases (MAPK) cascade, once it phosphorylates and inactivates K-Ras (88). On the other hand, PKC can activate the MAPK cascade by phosphorylating more downstream components, Raf-1 and MEK (92,94).

Physiologically, kinins are generally recognised as vasodilator oligopeptides with diuretic effects, playing a role in blood pressure control (69,95). For example, they exert such effects by stimulating production of nitric oxide synthase and nitric oxide in endothelial cells following release of Ca^{2+} from intracellular stocks (83). Besides, they are involved in both physiological and pathological conditions, mediating inflammation (70), pain (96), diabetes (71), cardiovascular diseases (72,73), renal and cardiac function(73,97), being essential for the proper electrophysiological functioning of the heart (98,99). Further, kinins have been long described as involved with protein synthesis (100) and cell division stimulation (70). More recently, Sheng *et al.* (101) reported anti-apoptotic effects exerted by B2R over endothelial cells subjected to hypoxia.

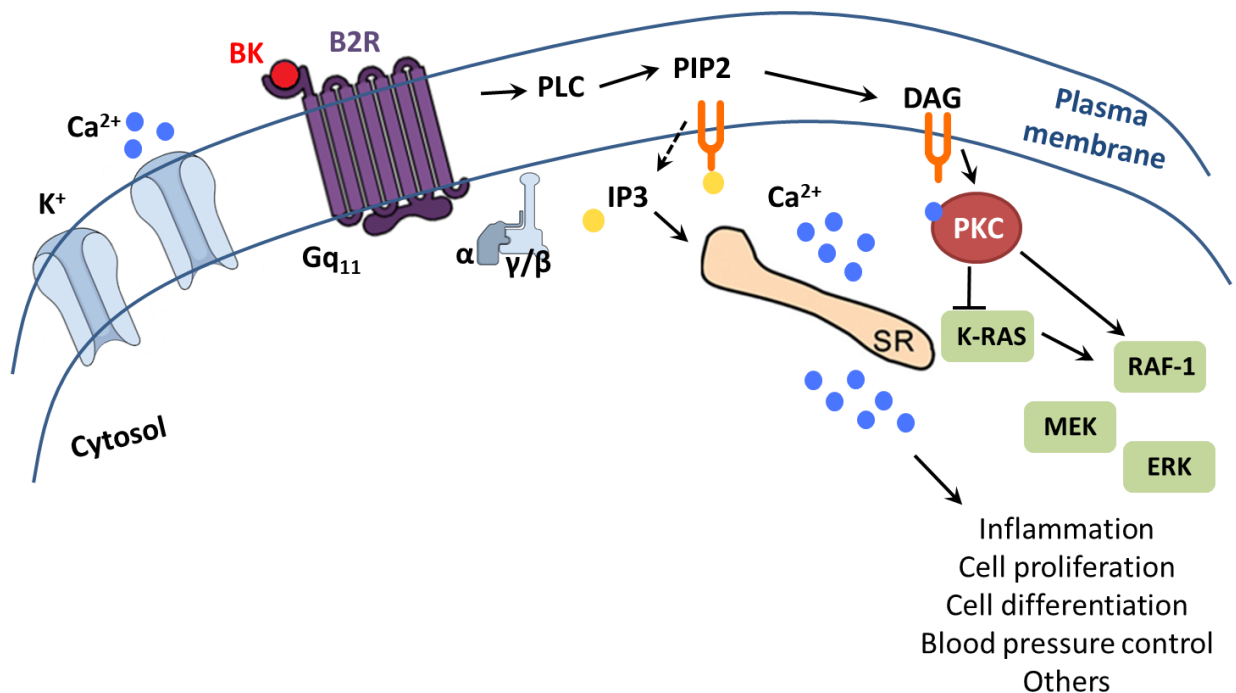


Figure 3. Schematic representation of signalling cascade triggered in response to B2R activation by bradykinin (BK). BK activates the membrane G-protein-coupled kinin B2 receptor, triggering activation of PLC, which catalyses the hydrolysis of PIP2 into DAG and IP3. IP3 diffuses to the cytoplasm and binds to IP3 receptors on the sarcoplasmic reticulum, triggering the release of Ca^{2+} . DAG remains in the plasma membrane and, together with Ca^{2+} , potentiates the activation of PKC. PKC phosphorylates various substrates, among them RAF-1, activating the MAPK/ERK signalling. Activation of B2R triggers a variety of downstream cellular processes, such as inflammation, blood pressure control, cell proliferation and differentiation.

In addition to being related to cell proliferation and survival, our group has thoroughly studied the role of kinin receptors in *in vitro* cell differentiation: studies using human and mice embryonic cells show that, following retinoic acid induction, embryonic bodies undergo neuronal differentiation, expressing augmented levels of both BK and functional B2R towards the end of the differentiation stimulus (74,75,77,79). Moreover, B2R has been linked to embryonic stem cells differentiation to keratinocytes (78).

A recent study from members of our group shows that BK and B2R possibly play a role in the *in vitro* differentiation of myoblasts towards skeletal muscle (80). In this work, Alves and collaborators report impaired skeletal muscle regeneration of B2R knockout mice that underwent induced lesion. In addition to this, they observe a reduction in the differentiation potential of the myoblast cell line C2C12 following B2R inhibition with HOE-140. Conversely, inhibition of angiotensin converting enzyme by captopril results in increased expression of markers of differentiated skeletal muscle cells. – possibly by augmenting the availability of BK. Moreover, converging results from the literature also support the notion that BK mediates myogenic differentiation from myoblasts (102).

The addition of BK to cardiac progenitor cells isolated from human heart biopsies regulates cell proliferation by promoting a transition into G2/M and S phase of the cell cycle (103). Moreover, differentiation of mouse ESC into cardiomyocytes can be attained following activation of IP3 receptors by nitric oxide (104), which, on its turn, is acutely produced in response to BK treatment (105).

Regarding cardiomyocytes electrophysiological properties, B2R has been implicated in controlling basic cardiac function by acting as modulator of membrane currents in guinea-pig atrial cells (106) and mice ventricular cells (98). Patch-clamp experiments conducted in these studies reveal that either addition of BK to the cells or knockout of the B2R promote

changes in AP profile, Ca^{2+} and K^{+} currents. Taken into the context of cardiomyocyte differentiation, B2R seems to be intricately involved in the physiology of cardiomyocytes, and could possibly also be involved in cardiac cells differentiation.

JUSTIFICATIVE

2. JUSTIFICATIVE

This work characterized the expression of maturation markers and functional properties of hiPSC-CM and investigated the role played by the kinin B2 receptor in hiPSC *in vitro* differentiation into cardiomyocytes. Based on this, this study sought attaining a bigger comprehension of differentiation and maturation processes and protocols. Ultimately, *bona fide* CM could be considered accurate *in vitro* models and contribute to multiple fields among cardiovascular diseases, such as cardiac disease modelling and *ex vivo* organ regeneration. In the clinic, a more rational drug design would promptly detect arrhythmogenic drugs. In addition to this, personalised therapies using patient-specific hiPSC-CM could potentially emerge from properly differentiated and characterized cells.

OBJECTIVES

3. OBJECTIVES

The main objective of this work was to evaluate the role played by kinin B2 receptor during the hiPSC differentiation into cardiomyocytes, regarding molecular and functional maturation.

3.1. Specific Objectives

- 3.1.1** Characterize, by RT-qPCR, the expression of *TNNI1*, *TNNI3* and *MYL2* throughout hiPSC-CM differentiation;
- 3.1.2** Characterize, by flow cytometry, the expression of skeletal (ssTnI) and cardiac (cTnI) protein isoforms of troponin I and MLC2v throughout hiPSC-CM differentiation.
- 3.1.3** Characterize the action potential of hiPSC-CM atrial, ventricular and nodal subtypes by whole-cell current clamp;
- 3.1.4** Verify the expression of B2R in differentiating hiPSC-CM and perform a dose-response curve of B2R activity by Ca^{2+} imaging and, based on that, define the treatment dose;
- 3.1.5** Evaluate, following B2R activation or inhibition during hiPSC-CM differentiation;
 - 3.1.5.1** The ratio of *TNNI1* and *TNNI3* expression throughout hiPSC-CM differentiation, by RT-qPCR;
 - 3.1.5.2** The expression levels of cTnI, ssTnI and MLC2v in obtained hiPSC-CM, by flow cytometry;

MATERIALS AND METHODS

4. MATERIALS AND METHODS

4.1. iPSC generation, differentiation and culturing

iPSC were derived from erythroblasts and fibroblasts and differentiated towards cardiomyocyte by the startup company PluriCell Biotech, in a 29-days protocol that consistently generates cardiomyocytes with over 90% purity. Differentiation was modulated by daily additions of 10 μ M or 1 μ M BK (Tocris Bioscience, United Kingdom), after the 5th day of differentiation (Fig.4). Alternatively, cells were treated for 5 or 15 minutes with 5 μ M of the B2R inhibitor Firazyr (Shire Pharmaceuticals, Ireland) - also known as HOE-140. After this time, cells received either 10 μ M or 1 μ M BK. The effect of B2R modulation on cardiomyocyte differentiation was compared to cardiomyocytes derived using the standard differentiation protocol established by PluriCell Biotech.

For electrophysiological analysis, 1x10⁵ viable cells were seeded on 35mm dishes coated with Geltrex® (Thermo Fisher, USA), using RPMI 1640 medium (Gibco, Ireland) supplemented with 1x B-27 (Thermo Fisher, USA) and maintained in an incubator at 37°C, 5% CO₂. For flow cytometry and RNA extraction, hiPSC-CM were cultured at high confluence on 12-well plates coated with Geltrex®.

Fig. 4 illustrates the timeline of hiPS-CM differentiation from hiPSC, as well as the timepoints on which each experimental analysis and drug treatments were conducted. hiPSC-CM were harvested on days 0, 5, 7, 15 and 30 of differentiation for gene expression analysis, on days 0, 5, 15 and 30 for analysis of protein markers by flow cytometry and on days 5 and 30 for protein analysis by western blot. In addition to this, electrophysiological analysis of cardiac APs were performed between days 32 and 47.

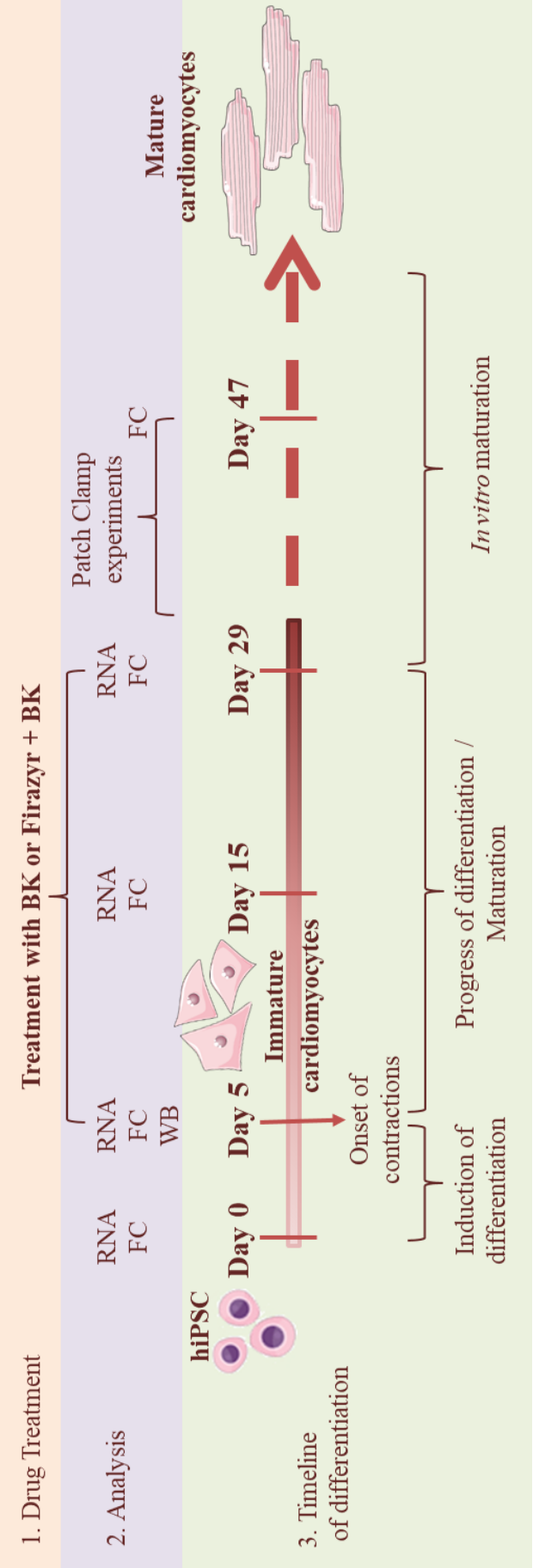


Figure 4. Timeline of hiPSC differentiation, experimental and drug treatment timepoints. The induction of cardiomyocyte differentiation from hiPSC lasted 5 days, after which spontaneous sarcomere contractions start. Cells remain in culture for further maturation until day 29th, the last day of the differentiation protocol established by PluriCell biotech. Alternatively, cells were kept in culture until day 47, being used for electrophysiological and flow cytometry experiments. Traced lines indicate that cells could theoretically be kept in culture indefinitely, seeking further maturation. Activation or inhibition of B2R with BK or Firazyr + BK was done between the 15th and 29th days of differentiation. Abbreviations: FC – flow cytometry, WB – Western Blot

4.2. RNA extraction and cDNA conversion

Total RNA was isolated from three biological replicates throughout cardiomyocytes differentiation (days 0, 5, 7, 15, 30) using Trizol reagent (Invitrogen Limited Paisley, Scotland, UK), according to manufacturer's instructions. In order to assess RNA concentration and purity, RNA was quantified in a spectrophotometer (NanoDrop ND-100 Spectrophotometer, Thermo Fisher, USA). RNA integrity was evaluated by an integrity 1% agarose gel. 2µg of total RNA were treated with DNase (Thermo Fisher, USA) for elimination of genomic DNA contamination (30 min at 37°C with further addition of 5mM EDTA for 10min at 75°C). 1µg of total RNA was converted into cDNA using RevertAid reverse transcriptase (Thermo Fisher, USA). For that, the mRNA template was annealed with 0.5mM Oligo dT (5min at 65°C) and, in sequence, 1x Revertaid Buffer, 0.5mM dTNPs, 2U/µl Ribolock (Thermo Fisher, USA) and H₂O DEPC-treated water were added to the reaction. Samples were incubated on an Applied Biosystems (Thermo Fisher, USA) thermocycler at 42°C for 60min and 70°C for 10min.

4.3. Conventional polymerase chain reaction (PCR)

The polymerase chain reaction (PCR) was employed in order to verify the specificity of primers designed for this study. Table I contains primer sequences used in this work and their respective amplicon sizes. All primers were designed on the NCBI Primer-Blast online tool, spanning different exons, in order to avoid amplification of genomic DNA. Sequence design was based on the consensus cDNA sequences available on GenBank (<http://www.ncbi.nlm.nih.gov>).

All samples received 1x Taq Polymerase Buffer+NH₄SO₄-MgCl, 1mM MgCl₂, 0.4mM dNTPs, 50-100ng of cDNA and 400nM of each primer. The PCR reactions were carried on the thermocycler according to the following protocol: 3min at 95°C for initial

double strand separation and 35 cycles of: 0:40min at 95°C, 0:50 min at 60°C for primer annealing, 2 min at 72°C for primer extension, with final 2 min at 72°C. The PCR products ran, for 60 minutes, on a 1.5% agarose gel. The gel was stained with 1x Sybr Green Nucleic Acid Gel Stain (Thermo Fisher, USA) and photographed under ultraviolet light.

4.4. Semi-quantitative reverse transcription real time PCR (RT-qPCR)

The efficiency of each primer pair on RT-qPCR was assessed by a standard curve with cDNA concentrations ranging from 50 - 3.25ng/μL on 1:1 dilutions. Primer concentration was kept constant at 160nM and 1x Power Sybr Green Master Mix (Thermo Fisher, USA) was added to the reaction. Relative gene expression quantification was performed in duplicates using a final volume of 10 μL per well, 160nM primer concentration, 0.62nmoles cDNA and 1x Power Sybr Green Master Mix. Non-template controls (NTC) were included for each primer pair. Only primers with efficiencies between 90 – 110% were used in this study.

RT-qPCR reactions were carried on a StepOne™ Plus Real-Time PCR System (Thermo Fisher, USA) and consisted of 40 cycles of 0:20min at 95°C and 0:20 min at 60°C. Data was acquired and analysed on StepOne™ Plus Real-Time PCR software (Thermo Fisher, USA). Arbitrary units of each gene expression were obtained by the $2^{-\Delta\Delta C_t}$ formula. *RPLP0*, *PPIA* and *SRP14* endogenous genes were used for the normalization of target genes expression. Data is expressed as “fold change” in relation to experimental controls.

Table I: Primer sequences for each gene analysed, respective primer sizes and amplicon sizes.

Gene (Accession Number)	Sequence	Primer size	Amplicon Size
<i>TNNI1</i> (NM_003281.3)	F: TGCCGGAAGTCGAGAGAAAA R: GTCGTATCGCTCCTCATCCA	20 20	245
<i>TNNI3</i>	F: CCTTCGAGGCAAGTTTAAGCG	21	155

(NM_000363.4)	R: GGTTCCTTCTCGGTGTCCT	21	194
<i>MYL2</i>	F: TTGGGCGAGTGAACGTGAAAA	21	
(NM_000432.3)	R:CCGAACGTAATCAGCCTTCAG	21	160
<i>SRP14</i>	F: CGTCGGGCAGCGTCTATATC	20	
(NM_003134.5)	R: TCCTTGGAGCTCACCACAGT	20	170
<i>PPIA</i>	F: GGGGCCGAACGTGGTATAAA	20	
(NM_021130)	R: GTCTGCAAACAGCTCAAAGGAG	22	

4.5. Saline Solutions

4.5.1. Patch clamp saline solutions

Saline solutions were prepared using ultrapure deionized water. Extracellular saline solutions consists in 1.8mM CaCl₂, 15mM Glucose, 15mM HEPES, 5.4mM KCl, 1mM MgCl₂, 150mM NaCl, 1mM Na-Pyruvate and adjusted to pH 7.4 with NaOH. Intracellular solutions were prepared using 2mM CaCl₂, 5mM EGTA, 10mM HEPES, 150mM KCl, 5mM MgATP and 5mM NaCl. pH was adjusted to 7.2 using KOH. Solutions were filtered with 0.2 µM filter and aliquots stored at -20oC.

4.5.2. Ca²⁺ imaging

Saline solutions were prepared using ultrapure deionized water. Extracellular saline “Tyrode’s” solution consists in 1.8mM CaCl₂, 10mM Glucose, 5mM HEPES, 5mM KCl, 1mM MgCl₂, 0.4mM KH₂PO₄ and 140mM NaCl. pH was adjusted to 7.4 with NaOH. Solutions were filtered with 0.2 µM filter and aliquots stored at -20°C. An alternative version of Ca²⁺-free Tyrode’s solution was prepared with substitution of 1.8mM CaCl₂ by 1.8mM extra MgCl₂.

4.6. Whole-cell patch-clamp

Medium from dishes containing cardiomyocytes were exchanged for extracellular saline patch-clamp solution. Recording pipettes with resistance of 2-4M Ω were pulled on the day of each experiment and backfilled with intracellular solution. A gigaseal (resistance $\geq 1\text{G}\Omega$) between the pipette and the cells was created, and any holding voltages or currents removed. The amplifier mode was switched from voltage-clamp to current-clamp and spontaneous action potential (AP) activities were recorded continuously on gap-free mode. AP kinetics parameters illustrated in Fig.1 were analysed, and include: resting membrane potential (RMP), peak, action potential duration at 50% and 90% of the initial resting potential (APD50 and APD90), maximum rate of depolarization (dV/dt_{\max}) and action potential amplitude. The aforementioned parameters were used to support the classification of each cell into ventricular, atrial and nodal types. Recordings were performed at room temperature using a Axopatch 200B amplifier (Molecular Devices, CA, USA), digitized, stored and analysed using a Digidata 1440a and pCLAMP software (Molecular Devices, CA, USA). AP parameters are presented as mean \pm standard error (SE).

4.7. Measurement of changes in free intracellular Ca^{2+} ($[\text{Ca}^{2+}]_i$) concentration

iPSC-CM were stained, for 40 minutes, at 37°C, with 5 μM Fluo 4-AM (Thermo Fisher, USA) and 0.02% pluronic acid (Thermo Fisher, USA in RMPI-1640 medium (Thermo Fisher, USA). Cells were washed three times in Tyrode's solution and at least 15 minutes were allowed for complete de-esterification of Fluo 4-AM. Measurements of BK-induced oscillations in free intracellular Ca^{2+} concentration analysis were performed in experimental and biological triplicates on Ca^{2+} -free Tyrode's solution, using an inverted fluorescence microscope (Nikon Instruments, Japan), under an argon 488nm laser. Each cellular preparation was imaged for 5min at a rate of 1 frame per second. Relative fluorescence is

expressed as $\Delta F/F_0$, which is the ratio between fluorescence in the presence of agonist or antagonist (ΔF) and basal fluorescence (F_0), as described by Nascimento *et al.* (77). Data was acquired and analysed on NIS-Elements Software (Nikon Instruments, Japan). At least 110 cells were used for each analysis.

4.8. Protein isolation and Western Blot

Cells on days 5th day of differentiation were collected following enzymatic harvesting and the cell pellet was frozen at -80°C until further processing. Cell pellets were dissociated with cold 1X RIPA buffer (Thermo Fisher, USA) supplemented with 1% serine-threonine proteases and tyrosine phosphatases inhibitors cocktail (Sigma-Aldrich, USA). All samples were centrifuged at 12.000 g, 10 min at 4°C. Protein samples were quantified by the bicinchoninic acid assay (BCA) method (Thermo Fisher, USA) and 20µg of total proteins were separated on 8-12% SDS-polyacrylamide gel, and then transferred to a nitrocellulose membrane. The membrane was blocked at least 1h at 4°C in 5% fat milk or 5% BSA in TBS-T and probed with primary antibodies overnight at 4°C.

On the next day, the membrane was washed 3 times with TBS-T (50 mM Tris-Cl, pH 7.6; 150 mM NaCl) followed by 1h incubation at room temperature with horseradish-peroxidase-conjugated secondary antibody (Millipore, USA). The membranes were exposed to Clarity Western ECL substrate (Bio-rad, USA) for 5 minutes and the signal was recorded on Uvitec (Cleaver Scientific, UK). Please refer to Table II for titrations and catalogue numbers of primary and secondary antibodies.

Table II: List and of antibodies employed in western blot experiments

Antibody	Host	Dilution	Company	Catalogue Number	Secondary Antibody	Exposure Time
B2R	Rabbit	1:500	Bioss	BS-2422R	Horseradish-peroxidase anti-rabbit (1:10.000) - Millipore	1:00 min
Gapdh	Mouse	1:5.000	Abcam	Ab8245	Horseradish-peroxidase anti-mouse (1:10.000) - Millipore	0:05min

Band intensities were measured and quantified by the Uvitech Cambridge software (Cleaver Scientific, UK) . For semiquantitative analysis, all antibodies signal intensity were analyzed and corrected in relation to GAPDH.

4.9. Flow cytometry

Expression levels of ssTnI, cTnI, MLC2v, and ACTN2 were assessed by flow cytometry. Differentiated cardiomyocytes were enzymatically detached from flasks, and mechanically dissociated to a single cell suspension. Cells were fixed using 1ml of fixative solution (1.25% PFA, 1% methanol) for 30 min, at 4°C and permeabilized with blocking solution consisting of 0.1% saponin (Sigma Aldrich, USA) and 10% FBS. Blocking solution was also used to dilute all antibodies in flow cytometric experiments.

Cells were co-stained, for 30 minutes, at 4°C, with rabbit anti-ssTnI primary antibody (Thermo Fisher, USA) and mouse anti-cTnI primary antibody conjugated with Alexa Fluor 647 (BD Biosciences, USA). Alternatively, cells were co-stained with rabbit anti-MLC2v primary antibody (Abcam, United Kingdom) and mouse anti-ACTN2 primary antibody. All secondary antibodies had Alexa Fluor fluorophores (Thermo Fisher, USA). Donkey anti-rabbit Alexa Fluor 488 secondary antibody (1:2000) was used against rabbit anti-ssTnI and against rabbit anti-MLC2v. Donkey anti-mouse Alexa Fluor 647 secondary antibody (1:3000) was used against mouse anti-ACTN2. Please refer to Table III for antibody titrations and

respective catalogue numbers. Cells were washed with 0.1% saponin 2% FBS two times following primary antibody incubation and one time after secondary antibody incubation. Cells were re-suspended in PBS 5% bovine serum albumin for analysis on flow cytometer.

Primary and secondary antibodies were titrated using hiPSC as negative controls. Flow cytometry measurements were performed using Attune (Life Technologies, USA). 638nm helium-neon and 488 nm argon lasers were used for fluorochromes excitation. At least thirty-five thousand events were acquired per sample and data was analysed using Flow Jo software (Tree Star, 2013). Forward and side light-scatter gates were used to exclude doublets cells and debris. Expression of ssTnI, cTnI, MLC2v and ACTN2 were estimated based on fluorescence signals in comparison to the background fluorescence of respective unstained controls. Data is presented as mean \pm standard error (SE) of at least three biological replicates.

Table III: List of antibodies employed in flow cytometry experiments

Antibody	Host	Dilution	Company	Catalogue Number	Secondary Antibody
ssTnI	Rabbit	1:1000	Sigma Aldrich	701585	Donkey Anti-Rabbit 488 1:2000
cTnI	Mouse	1:500	BD Biosciences	564409	Conjugated in 647
MLC2v	Rabbit	1:1000	Abcam	ab79935	Donkey Anti-Rabbit 488 1:2000
α-Actinin	Mouse	1:1000	Abcam	ab9465	Donkey Anti-Mouse 647 1:3000

STATISTICAL ANALYSIS

5. STATISTICAL ANALYSIS

The results of all experiments are presented as mean \pm standard error of at least three independent replicates. GraphPad Prism 5.0 software (GraphPad Software, USA) was used for statistical analysis. Data normality was evaluated by quantile-quantile plots. Normal data were analysed by Student's T-Test (if only between two groups) or Analysis of Variance (ANOVA) (if three or more groups), followed by Tukey's multiple comparison test. Non-normal data was analysed by non-parametric Kruskal Wallis test and Dunn's Multiple Comparison test. An alpha level of 0.05 was set as the significance level for this study.

RESULTS

6. RESULTS

6.1. Characterization of *TNNI1* and *TNNI3* expression throughout hiPSC-CM differentiation.

It is known that the genes that encode for the inhibitory subunit of the troponin complex are differentially expressed during development: while *TNNI1* accounts for the expression of the skeletal TnI isoform in fetal cardiomyocytes, *TNNI3* is only expressed on mature myocytes, resulting in the predominance of the cardiac TnI protein isoform (54,57).

In order to characterize the time-dependent shift on the expression of *TNNI1* and *TNNI3* on the hiPSC-CM used in this work, the relative expression of these genes was quantified on days 0, 5, 7, 15 and 30 of cardiac *in vitro* differentiation, by RT-qPCR (Fig.5).

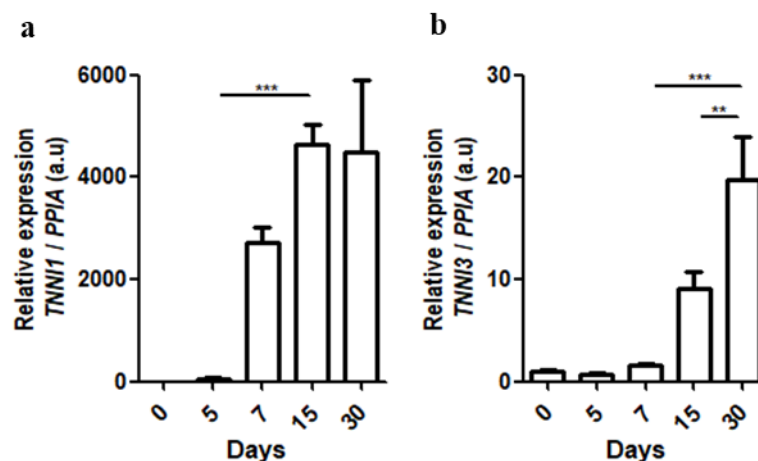


Figure 5. Relative expression of *TNNI1* and *TNNI3* genes by RT-qPCR throughout cardiac *in vitro* differentiation. (a) Relative expression of *TNNI1* gene normalized by *PPIA* on days 0, 5, 7, 15 and 30 of differentiation. (b) Relative expression of *TNNI3* gene normalized by *PPIA* on days 0, 5, 7, 15 and 30 of differentiation. N = 3 independent differentiations, each with experimental duplicates. Statistical Analysis: 1-WAY ANOVA and Tukey's multiple comparison test. **p<0.01; ***p<0.001

It is possible to observe that neither *TNNI1* nor *TNNI3* are highly expressed up to the 5th day of differentiation, as these cells still likely present a pluripotent or cardiac precursor phenotype, and do not yet present sarcomere contractions (data not shown). *TNNI1* expression increases 1000-fold between the 5th and 7th days of differentiation, reaching its peak after two

weeks of differentiation, after which it remains constant or slowly starts decreasing (Fig.5a). *TNNI3* expression, on the other hand, increases steeply from the 7th day on (Fig.5b). As *TNNI3* expression was only assessed until the 30th day of differentiation, it is not possible to know whether it would keep increasing or whether it would soon stabilize. This suggests that the hiPSC-CM model employed throughout this work presents the time-dependent shift between *TNNI1* and *TNNI3* gene expression described by Bedada *et al.* (57).

6.2.Characterization of ssTnI, cTnI, ACTN2 and MLC2v protein expression throughout hiPSC-CM differentiation.

ssTnI and cTnI co-expression throughout differentiation was assessed on days 0 (undifferentiated hiPSC), 5, 15 and 47, by flow cytometry (Fig.6a,c). It is possible to notice that neither isoforms of troponin I are expressed on undifferentiated iPSC, which confirms the antibody specificity to cardiomyocytes (Fig.6a). On the 5th day of differentiation, only 27% of cardiomyocytes express, on average, at least one troponin isoform, which mostly results from a co-expression of both isoforms. Analysis of alpha-actinin (ACTN2), another muscle sarcomeric protein revealed that, indeed, only 63% \pm 9.3% of the cells were committed to a muscle phenotype at this point (Fig.7b,d).

hiPSC-CM on the 15th day of *in vitro* differentiation are marked by 91.2% \pm 1.3% ssTnI and cTnI co-expression (Fig.6c) and ACTN2 levels superior of 95% (Fig.6d). This indicates that, at this point, the almost totality of cells have fully committed to a cardiac muscle phenotype, representing a more mature phenotype in comparison to hiPSC-CM on day 5 ($p<0.01$). Nevertheless, 30 more days in culture have not resulted in any significant shift towards the direction of cTnI single expression in detriment of ssTnI expression ($p=0.51$) (Fig.6 a,c). This suggests that these cells can still be considered immature and could benefit from strategies that seek inducing their *in vitro* maturation.

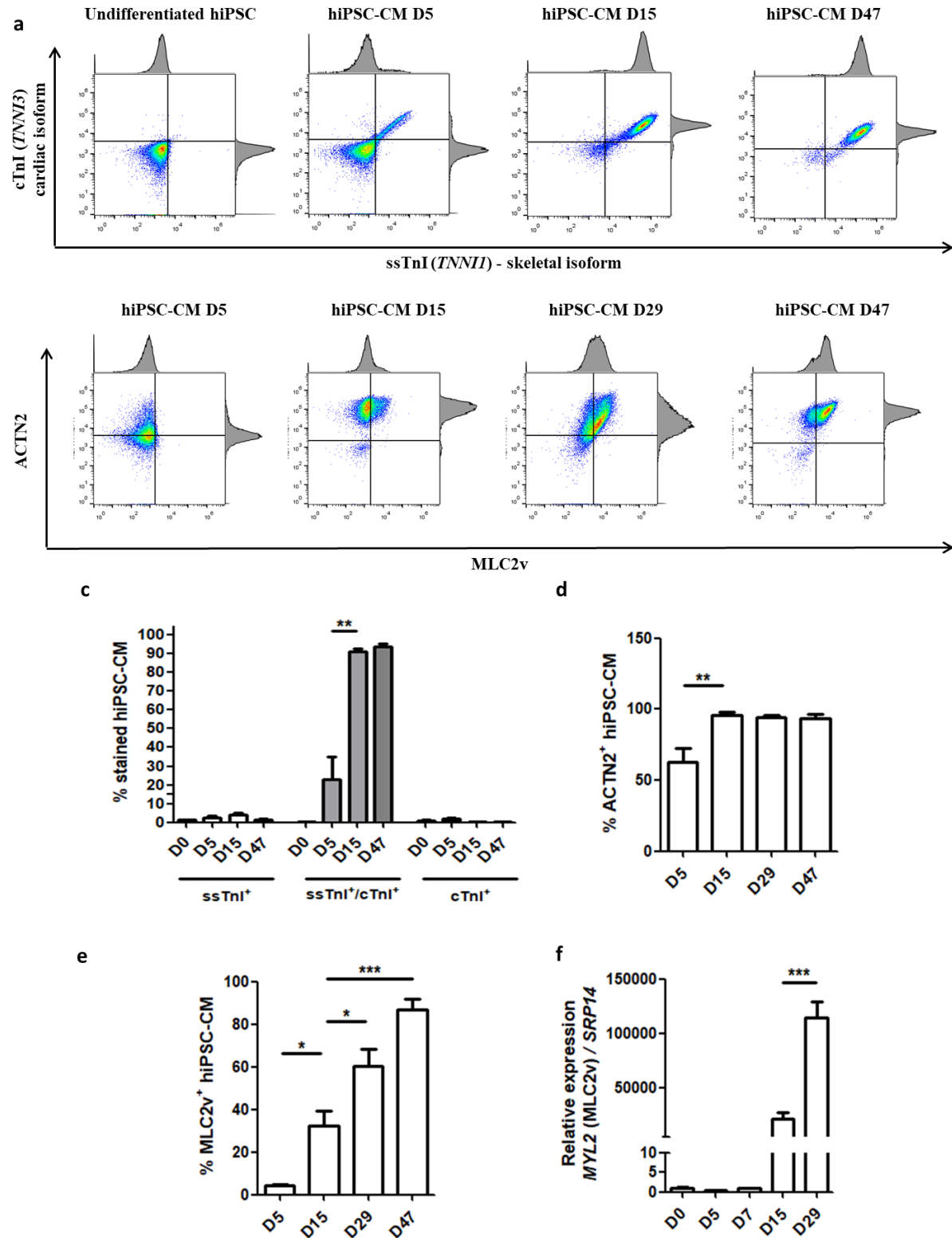


Figure 6. Co-expression of ssTnI and cTnI or MLC2v and ACTN2 in different timepoints of hiPSC differentiation by flow cytometry. hiPSC were induced to differentiate into cardiomyocytes and analysed on days 0 (undifferentiated hiPSC), 5, 15 and 47 regarding ssTnI and cTnI co-expression or MLC2v and ACTN2 co-expression. (a) Representative flow cytometric plots of ssTnI and cTnI co-expression on days 0, 5, 15 and 47 of differentiation. (b) Representative flow cytometric plots of MLC2v and ACTN2 co-expression on days 0, 5,

15 and 47 of differentiation. c) Quantification of hiPSC-CM single stained for ssTnI or cTnI or double stained for both troponin I isoforms. d) Quantification of hiPSC-CM single stained for ACTN2 or (e) for MLC2v. (f) Relative expression of *MYL2* gene (which encodes for MLC2v) normalized by expression rates of *SRP14* on days 0,5,7,15 and 30 of differentiation. N = 3. Results are expressed as mean \pm SE. Statistical analysis: 1-WAY ANOVA and Tukey's multiple comparison test. * $p < 0.05$, ** $p < 0.01$ and *** $p < 0.001$.

The analysis of the ventricular marker MLC2v throughout differentiation was also performed (Fig.6b,e,f). It is possible to verify that the expression of MLC2v increases linearly as differentiation progresses ($p < 0.001$). While less than 5% of the cells express MLC2v on the 5th day of differentiation (around the onset of beating), the expression of such marker reaches $86.8\% \pm 5.0\%$ of the population on day 47, with intermediate stages of MLC2v expression of $32.3\% \pm 7.0\%$ on day 15 and $60.5\% \pm 7.8\%$ on day 29. Additionally, these results are corroborated by the consistent increase in the expression of *MYL2*, the gene that encodes for this protein (Fig.6f) ($p < 0.001$).

6.3. Characterization of the action potential of hiPSC-CM

6.3.1. Classification of the proportions of atrial, ventricular and nodal subtypes

The electrophysiological classification of APs is considered the most reliable way to determine the fraction of each cardiomyocyte subtype in the population (38). In order to characterize the cardiomyocyte subtypes differentiated from hiPSC in this study as well as their electrical activity, single-cell spontaneous APs were recorded in gap free mode, for up to 5 minutes, using the whole-cell current-clamp technique. Mean AP curves were derived and analyzed regarding amplitude (mV), RMP (mV), dV/dT_{\max} (V/s), APD_{50} (s), APD_{90} (s) and frequency (Fig.1b). These parameters supported the single-cell AP classification between each cardiac subtype (ventricular, atrial and nodal). Representative APs from chamber-specific cardiac subtypes are depicted in Fig.7, in extended time scale (Fig.7 a,c,e) and in a 5-seconds interval (Fig.7 b,d,f).

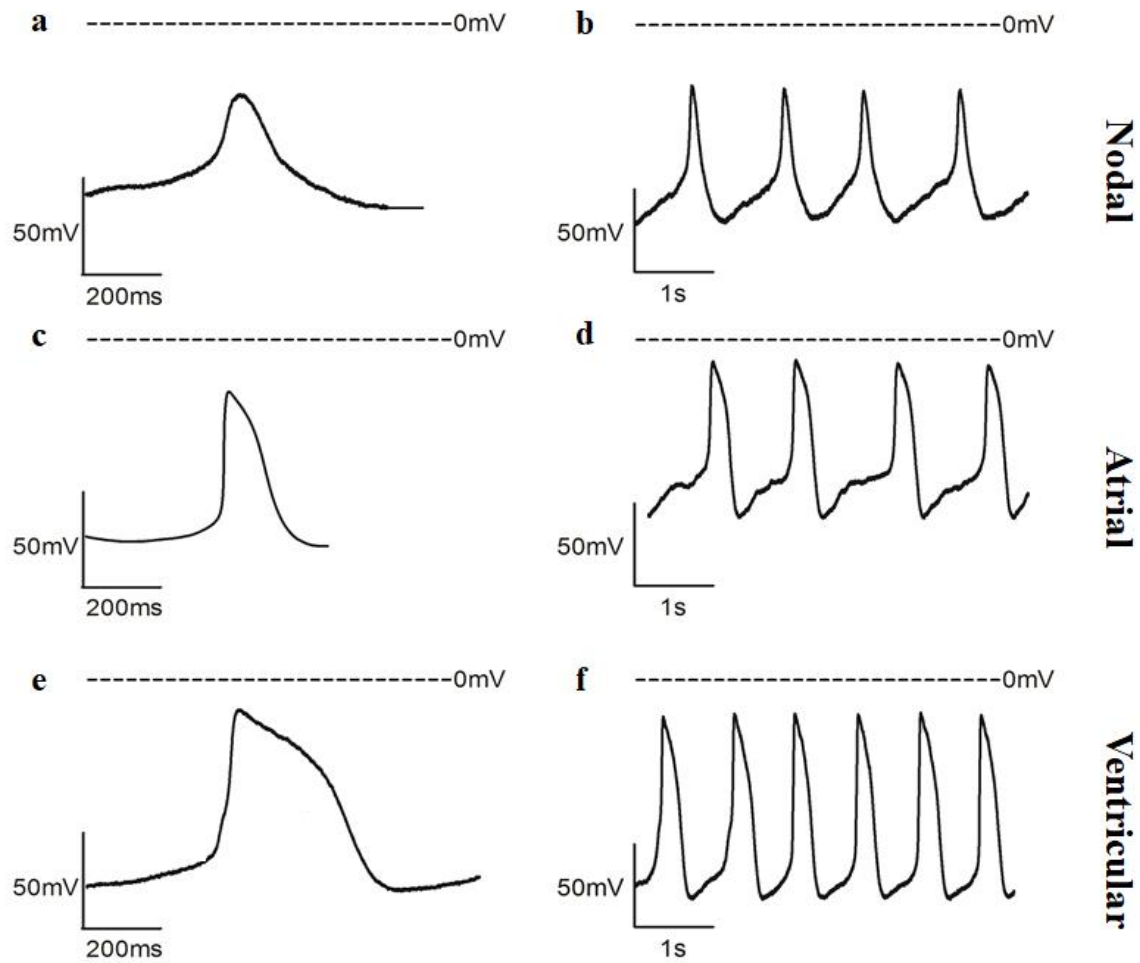


Figure 7. Representative subtype-specific AP traces in the hiPSC-CM population. Left: average APs in extended time scale. Right: subsequent APs in a 5 seconds interval. Traced lines indicate 0mV. It is possible to remark APs typical from nodal (a,b), atrial (c,d) and ventricular cells (e,f). N = 80 cells.

APs showing a blunt depolarization phase, a less negative and unstable RMP, slower upstroke velocity (dV/dt_{max}) and shorter amplitude were classified as nodal (Fig.7 a,b). This is consistent with the properties of such cells, once, although they are marked by poor contractility system, their relatively depolarized and unstable RPM result in the firing of repetitive action potentials (37).

CM presenting a deeper RMP and more pronounced dV/dt_{\max} were considered either atrial (if showing a shorter APD, Fig.7c,d) or ventricular (if displaying a marked plateau, Fig.7e,f).

As with molecular markers, it has been suggested that enhanced time in culture could induce maturation of the APs, in a sense that the expression of certain ion channels on the membrane could change, leading to variation in the kinetics of the action potential (66). Aiming to characterize if the proportions of the subtypes could change with enhanced time in culture, APs from hiPSC-CM were analysed in 4 different time windows spanning from the 33rd to the 48th day of differentiation (Fig.8). It is possible to remark that the proportions between nodal, atrial and ventricular-like cells changes with time in culture, being the variables “time” and “subtype” correlated ($p=0.02$). Still, as this observation *per se* was not sufficient to attest that time in culture was inducing maturation of hiPSC-CM electrical properties, the kinetic of APs on the aforementioned time window were also analysed.

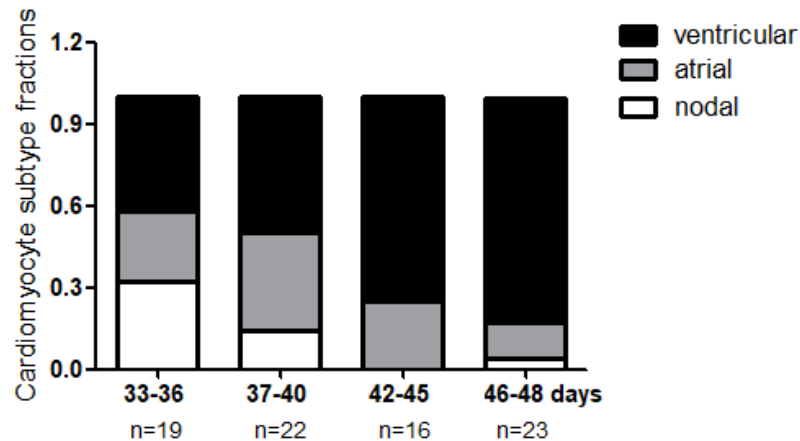


Figure 8. Distribution of cardiac subtypes in a hiPSC-CM population. Cardiomyocytes in different timepoints since the onset of differentiation were classified as ventricular, atrial or nodal-like. Single-cell subtype classification was performed based on AP kinetic parameters. N=80 cells. Statistical analysis: Pearson chi-square test, $p=0.02$

6.3.2. Analysis of time-dependent changes in the AP kinetics

The analysis of AP frequency (Fig.9a) revealed that nodal-like hiPSC-CM oscillate on a rather constant average rate of 26 APs/min, throughout the analysed timepoints. On the other hand, atrial-like and ventricular-like cells exhibit a tendency to progressively increase the AP firing rate, with more time in culture ($p=0.15$, $N=81$).

Another analysed feature was the maximum depolarization rate of the APs (dV/dT_{\max}), in the different subtypes and timepoints (Fig. 9b). Again, a tendency of dV/dT_{\max} increasing with time in culture can be observed in atrial-like cells ($p=0.10$, $N=81$), but not among nodal cells, nor among ventricular-like cells up to the 45th day of differentiation.

The average amplitude of nodal-like APs are significantly lower than atrial and ventricular-like APs ($p<0.01$ and $p<0.001$, respectively) (Fig.9c). In addition to this, atrial-like APs show amplitudes on average 20mV smaller than ventricular-like APs ($p<0.01$).

Similar considerations can be made regarding the duration of the generated APs (APD50 and APD90, figs. 9e,f): the AP from both nodal and atrial-like cardiomyocytes are significantly lower ($p<0.05$) than ventricular-like APs, although no clear correlation between differentiation age and APD can be made. In general, the longer APD in ventricular cells is attributed to a pronounced Ca^{2+} current component (I_{Ca}) in this cell type (Fig.1), as well as a more developed sarcoplasmic reticulum, where Ca^{2+} ions are stored during cardiac diastole (37).

Finally, the hiPSC-CM obtained in this study seem to present a stable RMP on the evaluated timepoints, with averages ranging between -77 mV and -92 mV. Although such parameters are rather close to the -85 mV RPM observed in the native myocardium (41), this does not explain the automaticity observed in these cells (normally associated with a more depolarized RMP, close to the threshold for AP firing (65)).

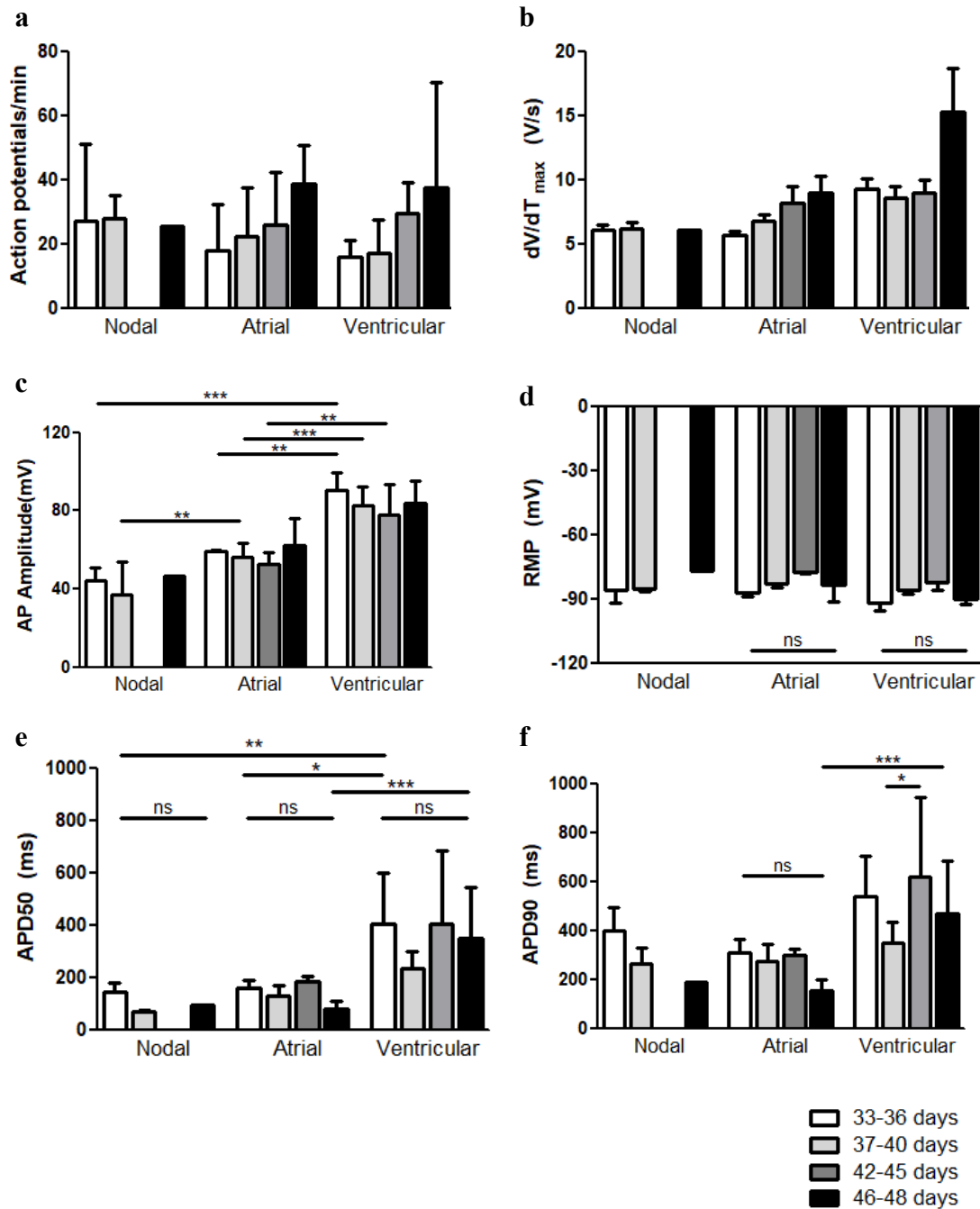


Figure 9. AP kinetic parameters from hiPSC nodal, atrial and ventricular subtypes in time intervals between the 33rd and 48th day of differentiation. (a) Frequency of spontaneous APs per minute (b) dV/dT_{max} (V/s); (c) AP Amplitude (mV); (d) RMP (mV); (e) APD₅₀(ms); (f) APD₉₀ (ms); (g) Membrane Capacitance (pF). Results are expressed as mean \pm SE. Statistical analysis: One-WAY ANOVA plus Tukey's Multiple Comparison Test (a,c-f) and Kruskal-Wallis test plus Dunn's Multiple Comparison Test (b). * $p<0.05$; ** $p<0.01$; *** $p<0.001$. N=3 independent differentiations, 81 cells.

6.4. Expression of B2R in differentiating hiPSC-CM, and verification of its responsivity to BK

In order to confirm that B2R was expressed in hiPSC-CM, its expression was verified by Western Blot. For this, total protein was extracted from hiPSC-CM samples on the 5th day of differentiation, quantified and subjected to a SDS-PAGE electrophoresis (Fig.10a). The analysis of the western blot membrane revealed protein bands with sizes correspondent to B2 receptor (44kDa).

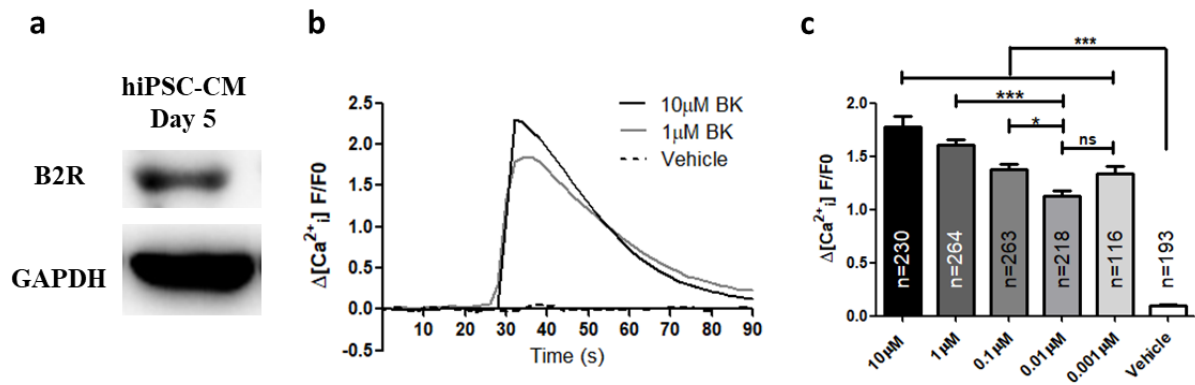


Figure 10. Analysis of B2R expression and activity in hiPSC on the 5th day of differentiation. (a) Representative western blot bands of B2R (44kDa) and the endogenous normalizer GAPDH. Total protein extracts from hiPSC-CM on the 5th day of differentiation were subjected to western blot analysis in order to verify the expression B2R. N=3 (b) Representative traces of relative variation in hiPSC-CM intracellular Ca^{2+} concentration in response to the addition of 1µM BK, 10µM BK or vehicle. hiPSC-CM on the 5th day of differentiation were stained with Fluo4-AM and imaged on a fluorescence microscope. (c) Relative oscillations in fluorescence following the addition of 10-fold decreasing BK doses (0.001µM - 10 µM) were quantified and compared to the addition of vehicle (injection water). Statistical Analysis: 1-WAY ANOVA and Tukey's multiple comparison test. N=1091 cells from 3 independent experiments.

The sole expression of the B2 receptor by the cell is not enough to indicate that the receptor stands active on the membrane, thus being liable to modulation by its ligand BK. Therefore, in order to verify this, a dose-response curve of BK on hiPSC-CM was performed.

As the pharmacological activation of the B2R triggers a metabotropic Ca^{2+} -dependent response, the activity of this receptor on the cellular membrane can be verified by Ca^{2+} imaging. Aiming to confirm that the B2R is present and active on the cellular membrane, a

dose-response relationship of BK on B2R activity was performed by Ca^{2+} imaging (Fig.10b,c). For that, iPSC were induced to cardiac differentiation, being stained with Fluo-4 AM and imaged on the 5th day of differentiation. The cell preparations received 10-fold increasing doses of BK (0.001 μM - 10 μM) or vehicle (Tyrode's solution) and the consequent variation in the cell fluorescence relative to the basal fluorescence ($\Delta[\text{Ca}^{2+}_i]/\text{F}/\text{F}_0$) was quantified (Fig.10c). As the Ca^{2+} signalling response triggered by B2R activation does not rely on Ca^{2+} present in the extracellular solution, but rather on the sarcoplasmic Ca^{2+} stocks, cells were imaged in a Ca^{2+} -free Tyrode's solution. This avoided spontaneous Ca^{2+} oscillations triggered by the Ca^{2+} induced Ca^{2+} release mechanism and potentially made the response more specific to B2R activation.

Figure 10b reveals that the addition of BK triggers a rapid Ca^{2+} oscillation which decreases over the following 60 seconds, while the addition of vehicle does not induce Ca^{2+} release from intracellular stocks. It is possible to observe that the B2R-induced mean variation in the cell fluorescence relative to the basal fluorescence ($\Delta[\text{Ca}^{2+}_i]/\text{F}/\text{F}_0$) is dose dependent (Fig.10c), and that BK doses as low as 1nM can lead to a 14-fold increase in the cellular fluorescence ($p < 0.001$). Previous works from our laboratory groups have used 1 μM BK to induce neural differentiation (75,77,79). As this peptide is not very stable in solution (half-life = 30s (85)) and aiming to induce the greatest possible response, we decided to first test the effect of 10 μM BK on *TNNI1* and *TNNI3* gene expression and ssTnI/cTnI protein expression.

6.5. Evaluation of hiPSC-CM phenotypes following B2R activation or inhibition during differentiation.

6.5.1. *TNNI1* and *TNNI3* expression following B2R activation with 10 μM BK or inhibition with Firazyr

hiPSC were induced to differentiate into cardiomyocytes using the conventional protocol standardized by PluriCell Biotech. Differentiating cells received daily additions of

10 μ M BK from the 5th day to the 15th day of differentiation. Alternatively, in order to establish if any biological variation was really being undertaken through the B2R and not through other means (such as activation of B1R), kinin B2 receptor activity was pharmacologically blocked with 5 μ M Firazyr for 5 minutes, followed by stimulation with 10 μ M BK.

Total RNA from each sample was collected and reverse transcribed into cDNA. *TNNI1* and *TNNI3* gene expression in BK and Firazyr + BK groups was compared to untreated controls. The results are depicted as fold change in relation to untreated controls (n = 2 independent *in vitro* differentiations) (Fig.11).

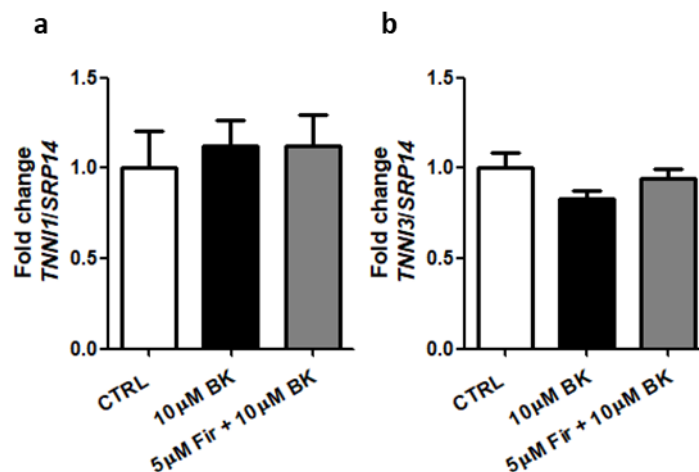


Figure 11. Relative *TNNI1* and *TNNI3* gene expression of hiPSC-CM differentiated in the presence of 10 μ M BK or subjected to B2R inactivation with 5 μ M Firazyr followed by stimulation with 10 μ M BK, in relation to control. (a) Relative *TNNI1* and (b) *TNNI3* expression in relation to unstimulated controls. Samples were collected on the 15th day of differentiation and *SRP14* was used as endogenous gene for normalizing expression rates. N=2 independent differentiations. Statistical Analysis: 1-WAY ANOVA and Tukey's multiple comparison test. P>0.05

The addition of 10 μ M BK following, or not, the pharmacological inhibition of B2R with 5 μ M Firazyr did not result in any significant change in *TNNI1* (Fig.11a, p=0.87) or *TNNI3* (Fig.11b, p=0.18) gene expression.

6.5.2. Expression of cTnI, ssTnI, MLC2v in hiPSC-CM following B2R activation with 10 μ M BK or inhibition with 5 μ M Firazyr

Protein expression levels of troponin I isoforms in hiPSC-CM differentiated until day 15 in the presence of 10 μ M BK or after B2R inhibition was assessed by flow cytometry. It can be observed that, on average, 90% of cells co-express the skeletal and cardiac isoforms in all conditions (Fig.12a,b), with no significant alteration in TnI expression in response to B2R activation nor inhibition ($p=0.81$).

The expression of MLC2v, a molecular marker of ventricular subtype, was assessed in hiPSC-CM after activation or inactivation of the B2R receptor. It is possible to remark, from fig.12c, a big variance in the percentage of MLC2v⁺ cells, among the two independent *in vitro* differentiation assays. Although the two performed independent differentiations yielded variable percentages of MLC2v⁺ cells (18% and 60%), the percentages of MLC2v⁺ cells in each treatment group, within each differentiation, remained constant ($p=0.99$).

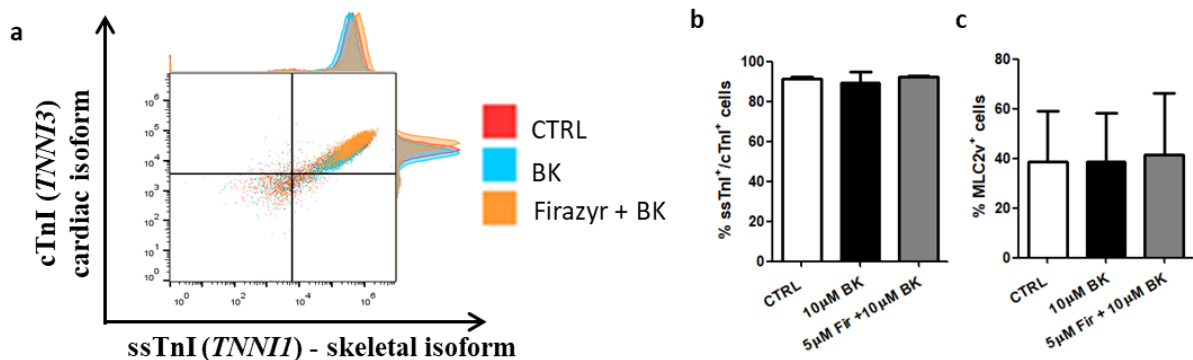


Figure 12. ssTnI/cTnI and MLC2v protein expression in hiPSC-CM differentiated in the presence of 10 μ M BK or subjected to B2R inactivation with 5 μ M Firazyr followed by stimulation with 10 μ M BK, on day 15 of differentiation. (a) Representative flow cytometry plots for cardiac and skeletal troponin I isoforms co-staining. Each treatment condition is depicted in one color and graphics are superposed. (b) Quantification of ssTnI⁺/cTnI⁺ cells in each treatment. (c) Quantification of MLC2v⁺ cells in each treatment condition. N=2. Statistical Analysis: 1-WAY ANOVA and Tukey's multiple comparison test. NS.

The lack of apparent effect of modulation of B2R activity on the maturation of hiPSC-CM led us to hypothesise that the B2 receptor could be undergoing desensitization/inactivation following stimulation with 10 μ M BK (refer to topic 7.3 on Discussion section for more details). Therefore, aiming to confirm the absence of biological effects on the expression of maturation markers or on the determination of the ventricular phenotype following activation or inhibition of B2R, we repeated the differentiation of hiPSC using a 10-fold lower dose of BK (1 μ M), increased the treatment with Firazyr to 15 minutes as well as prolonged the overall treatment duration until the 29th day of differentiation.

6.5.3. Gene and protein expression of troponin I isoforms and MLC2v following B2R activation with 1 μ M BK or inhibition with 5 μ M Firazyr

Cardiomyocytes were again differentiated from hiPSC, and this time, BK and Firazyr were daily added to the cells from the 5th until the 29th day of differentiation. A qualitative analysis of the three conditions under the microscope shows that the addition of BK or Firazyr has little or no effect over cellular morphology (Fig.13a). In addition to this, we verified that the different groups expressed ACTN2 in similar levels (Fig.13b,c $p=0.71$), consistently superior than 92%, suggesting that the drug treatments were not interfering with the efficiency of differentiation.

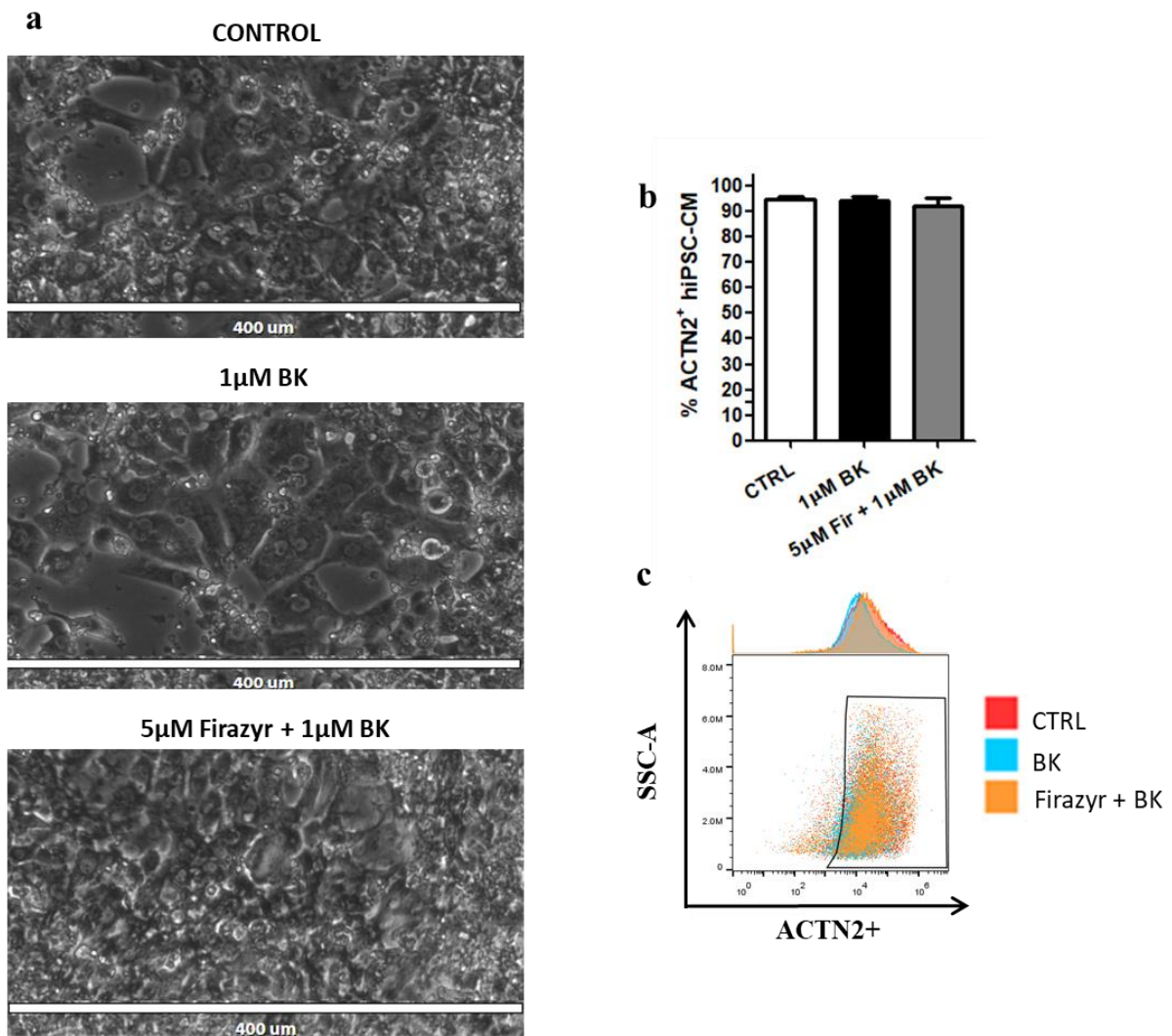


Figure 13. Effect of B2R activation or inhibition on the efficiency of cardiac differentiation from hiPSC. (a) Microscopy of untreated hiPSC-CM or cultured with 1µM BK or 5µM Firazyr+1µM BK. Cells were imaged during different stages of differentiation and a qualitative analysis showed no clear effect of BK or Firazyr treatment over the morphology of the hiPSC-CM or on their survival and ability to progress in differentiation. Scale bar = 400µm. (b) % of muscle cells (ACTN2⁺) in the population by the end of each treatment. (c) Representative flow cytometry plots of the expression of ACTN2 in each group. N=3. Statistical Analysis: 1-WAY ANOVA and Tukey's multiple comparison test. NS.

RNA was collected from untreated cells on day 5 and from the three treatment groups on day 29 (n=3). Analysis of *TNNI1* and *TNNI3* gene expression (Fig. 14a,b) reveals no significant variation in response to B2R activation or inhibition (p=0.43 and 0.93). Similarly, analysis of the protein levels of ssTnI and cTnI co-expression by flow cytometry (Fig.c,e) disclosed no variation in each treatment group (p=0.83).

Finally, expression of the ventricular marker MLC2v was also analysed by flow cytometry, under the described conditions. It is possible to remark that, on average, the performed treatments do not result in statistically relevant variations on the expression of MLC2v (Fig.14d, $p=0.92$).

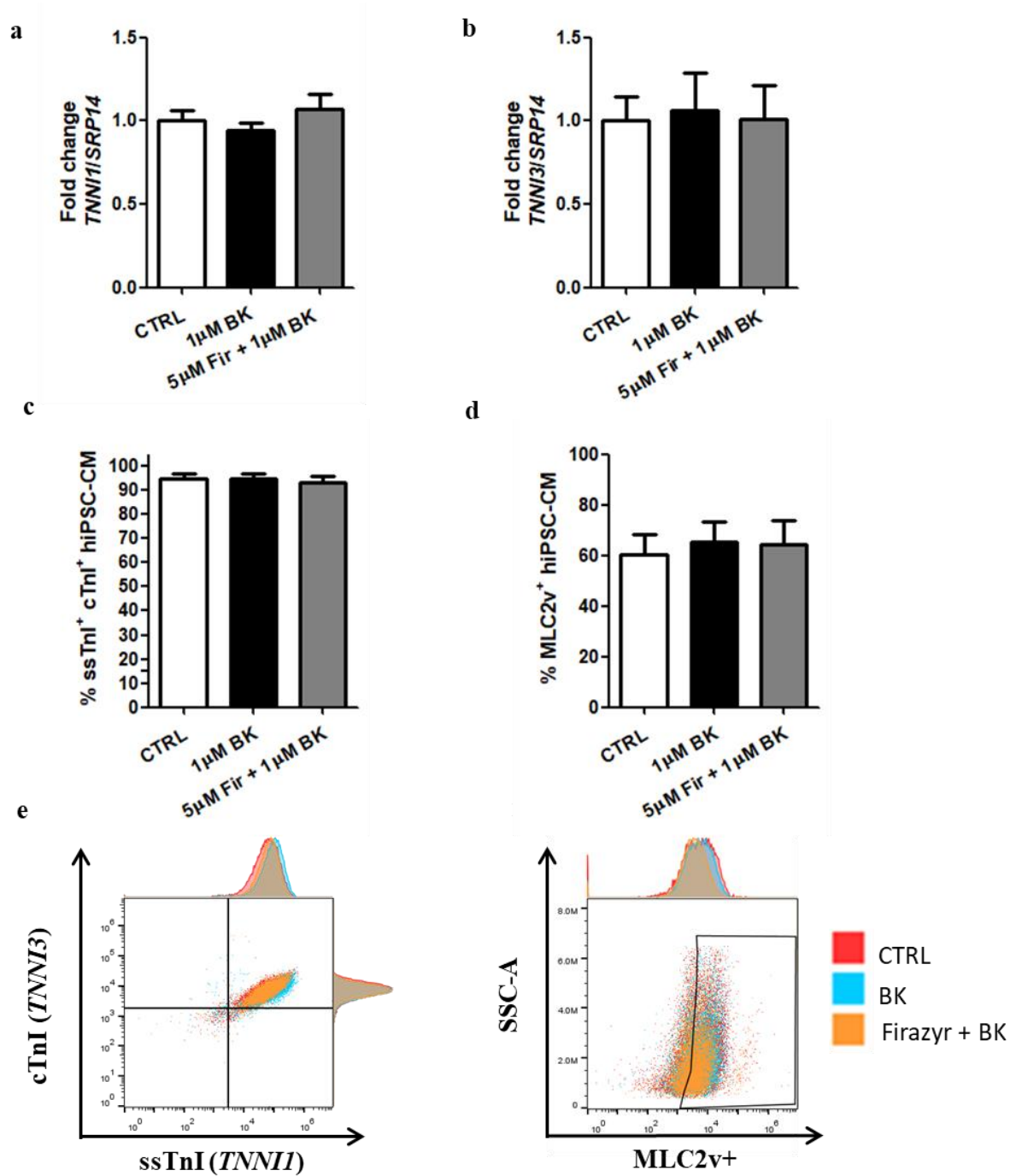


Figure 14. Gene and protein expression of troponin I isoforms and MLC2v following pharmacological activation of B2R with 1μM BK or blockade with 5μM Firazyr during

cardiac *in vitro* differentiation from hiPSC. (a) Relative *TNNI1* and (b) *TNNI3* expression in relation to unstimulated controls. Samples were collected on the 29th day of differentiation and *SRP14* was used as endogenous gene normalizer. N=4 (c) Quantification of hiPSC-CM double stained for both cardiac and skeletal troponin I isoforms or (d) single stained for MLC2v in each treatment group. (e) Representative flow cytometry plots for hiPSC-CM double stained with cTnI and ssTnI or (f) single stained with MLC2v. Each treatment condition is depicted in one color and graphics are superposed. N=3. Results are expressed as mean \pm SE. Statistical analysis: 1-WAY ANOVA and Tukey's multiple comparison test. NS.

We have been successful in characterizing the effect of time on the molecular and functional maturation of hiPSC-CM, as well as on the determination of the ventricular subtype. However, the involvement of B2R in cardiac maturation and subtype specification could, so far, not be evidenced.

DISCUSSION

7. DISCUSSION

7.1. Characterization of Troponin I gene and protein expression throughout hiPSC-CM differentiation.

Striking changes in the transcriptome of differentiating cells can be remarked during cardiogenesis (107). DeLaughter and collaborators (107) have performed a temporal analysis of gene expression during murine cardiogenesis with single-cell resolution, characterizing chamber-specific markers, and importantly, unravelling the temporal regulation of developmental gene expression programs. Among other important findings, they reiterated *TNNI3* as a gene with increasing expression as development progresses.

TNNI1 is first expressed in the cardiac tube, being co-expressed with *TNNI3* in late fetal/neonatal hearts (57). In the end of gestation, *TNNI3* transcripts start becoming more abundant than *TNNI1*, and the expression of the latter ceases completely only postnatally (54–57). In fact, it seems that the molecular regulation of this process occurs in both transcriptional and translational levels (56).

The analysis of *TNNI1* and *TNNI3* gene expression in this study revealed that these genes are concomitantly expressed throughout the *in vitro* differentiation of hiPSC-CM, being mostly expressed after the 7th day of differentiation (Fig.5). It is possible to remark that the time-dependent variation shift on *TNNI3* expression is more prominent, in a way that the relative abundance *TNNI1* in relation to *TNNI3* becomes smaller with time, corroborating the model that predicts the troponin isoform switch as differentiation progresses (57).

In the protein levels, the results obtained by our flow cytometry experiments confirm that neither TnI isoforms were expressed in undifferentiated hiPSC (Fig.6). Considering that under the present differentiation protocol cardiac contractions start between the 5th and 6th days of differentiation (data not shown), it seems reasonable to state that if sarcomeres are functional enough to contract, at least one TnI isoform must be present. Flow cytometry

results show that 5 days after induction to differentiation, an average of 22.8% of these cells already co-express both troponin I isoforms (Fig.6c). This observation is supported by the very low levels of *TNNI1* and *TNNI3* transcripts on 5-day old cardiomyocytes (Fig.5). Additionally, the onset of cTnI expression on 5-day old hiPSC shows that, from the first week of differentiation, hiPSC-CM are already transitioning from fetal to neonatal-like state – at least regarding these maturation markers.

Moving forward in the *in vitro* differentiation, hiPSC-CM go through a stage, in which over 90% of the cells co-express both troponin I isoforms, perduring from day 15 to at least day 47 (Fig.6c). It seems, thus, that prolonged time in culture is an insufficient approach to generate relevant amounts of cTnI⁺/ssTnI⁻ subpopulations.

In the literature, the expression of *TNNI3* is reported to increase following *in vitro* attempts to induce maturation of PSC-CM, such as by employing electrical stimulation (4), biomaterials (67), biophysical (108) and biochemical cues (109). Upregulated cTnI protein expression has also been reported following experimental approaches to induce PSC-CM maturity, for instance, by means of co-culturing with endothelial cells (110), by blocking Wnt signalling with small molecules (109), employing biomaterials (67) and even by transplanting these cells into the heart of infarcted mice, in a way to induce *in vivo* maturation (111).

In fact, although the observed increase in *TNNI3*/cTnI levels goes in line with the improvement of other maturation markers (e.g. cardiomyocyte sarcomere ultrastructure, Ca²⁺ handling and electrophysiological properties), studies show that *TNNI3* remains about 23 times less expressed in 2 months-old hiPSC-CM than in the native human heart (34). Considering this information and our results, extending *in vitro* culture into even longer periods of time could be prohibitive in terms of costs, and maybe still insufficient to reach fully mature hiPSC-CM which can be used for cell therapy or other clinical applications. Still,

the analysis of the differential expression of troponin I isoforms seemed like a valid approach to assess hiPSC-CM maturation throughout the next steps of the present work.

7.2.Characterization of the electrophysiology of hiPSC-CM

7.2.1. Analysis of the proportions of atrial, ventricular and nodal subtypes

The electrophysiological analysis of PSC-CM action potentials is the gold standard to identify the different cellular subtypes that are generated by the currently developed differentiation protocols (38,39). The results from this study suggest a time-dependent variation in the proportions of each cardiac subtype that comprise the total hiPSC-CM population. Following the end of the 30-day differentiation protocol balanced proportions of the three cardiac subtypes can be observed (Fig.8). However, it is possible to notice that two more weeks in culture culminate in a shift in the population composition, towards the predominance of the ventricular phenotype and an almost absence of nodal-like APs.

It is interesting to see that these results are corroborated by the analysis of the expression of MLC2v (Fig.6e) and of its correspondent gene (*MYL2*, Fig.6f). In fact, the time-dependent increase in the expression of this marker occurs in similar rates to that observed in the electrophysiological experiments. Unfortunately, due to our inability to standardize working antibodies for atrial and nodal subtypes during this project, it was not possible to report whether such shift can also be verified in the molecular level.

A similar observation had been previously performed by Ben-Ari and collaborators (64), who reported the decrease in the expression of the proposed nodal marker HCN4 and concomitant increase in the expression of atrial and ventricular MLC2a and MLC2v markers on day 60 of differentiation in comparison to day 30. Regarding electrophysiological properties, the same authors report a time-dependent increase in dV/dT_{\max} , amplitude and AP

duration on older hiPSC-CM, which are hallmarks of the ventricular AP. The authors also show that such shift from nodal to atrial/ventricular phenotypes includes intermediate transitional populations, and conclude that the electrophysiological signature of a cell is not fixed throughout development – that means, it is not genetically predetermined in the cardiac precursors. Instead, they suggest that cells could potentially interconvert between phenotypes in response to unknown environmental cues.

However, it could be argued that the parameters that support AP classification into different subtypes would only be valid during a limited period of development, rather than throughout the entire cardiogenesis, with eventual (and confounding) overlapping of AP properties (112). Moreover, it has been proposed that the AP kinetic parameters fail in efficiently clustering differentiated hiPSC-CM into discrete subpopulations (64).

Ideally, we propose that a more robust subtype classification could be attained by performing electrophysiological analysis of APs in hiPSC-CM engineered to express fluorescent constructs for subtype-specific markers. Another (rather laborious) way to combine molecular and functional data would be to perform single-cell qRT-PCR of cells patched immediately after current-clamp characterization of APs. Both methods would allow verifying whether the expression of subtype-specific molecular markers matches AP profiles, or, vice versa – if cells displaying a specific AP profile simultaneously express molecular markers of a second (or third) cellular subtype. Ultimately, such experiments would provide bigger insights into the mechanisms of subtype fate specification as differentiation progresses.

7.2.2 Analysis of time-dependent variations in AP kinetics

The existence of spontaneous contractions on *in vitro* differentiated cardiomyocytes is an indicator that these cells present a relatively functional contractile apparatus, that relies on the time-coordinated functioning of voltage-gated ion channels and of a sarcoplasmic

reticulum which not only bears massive Ca^{2+} stocks but also can respond to intrinsic mechanisms that coordinate the release and reuptake of these ions (113).

The functionality of ion channel matures as *in vivo* cardiogenesis progresses (113–115) and this culminates in electrophysiological alterations on AP kinetic parameters (112). Peinkofer and co-workers (112) performed a systematic analysis of the action potentials of atrial and ventricular heart slices obtained from a spectrum of seven developmental ages encompassing embryonic, newborn and adult hearts. They used this data to classify the murine iPSC-CM APs into more defined developmental stages and verified time-dependent alterations in most AP kinetic parameters (RMP, APD, Amplitude, dV/dT_{\max}).

The morphology of APs is the result of a net balance of all ion currents that enter and leave the cell (116). Because of this, several studies have characterized the expression and activity of ion channels in *in vitro* differentiated cardiomyocytes and reported all inward and outward currents depicted in Fig.1a, except from the I_{K1} current, which is often absent or present on very low densities on PSC-CM (65,113,117–120). Although the study of ion currents is important to assess the functionality of hiPSC-CM and validate their use as platform for *in vitro* drug testing, such characterization was beyond the scope of this project. Nevertheless, as the AP shape and kinetic parameters are consistent with those observed in the literature (42,117,118,121,122), it seems reasonable to assume that it is properly regulated by the ion channels that most commonly coordinate the cardiac AP.

The hiPSC-CM differentiated in this study fire APs in a rate ranging from 16-38 AP/min, on average (Fig.9a). This rate is comparable to that observed in other studies, which report 21-130 beats per minute (118,123). Variations on the average AP firing rate as a consequence of more prolonged time in culture have been reported, although the magnitude and direction of these observations are not necessarily consistent among studies (123). For

instance, Sheng and collaborators (118) compared the electrophysiological properties of PSC-CM on day 20 and 60 of differentiation and report an increased firing AP rate on day 60 in comparison to day 20. In the present study, atrial and ventricular-like hiPSC-CM have demonstrated a tendency ($p=0.15$) to increase average firing rate throughout 2 weeks in culture.

It should not be left unnoticed that, on the native myocardium, the only cells that fire spontaneous APs are the pacemaker cells located in the sinoatrial node, thus being responsible for the rhythm of each heartbeat. The RMP in non-pacemaker cardiomyocytes is kept stable by the I_{K1} current, a K^+ inward rectifier current that runs through the Kir2.1 channel encoded by the gene *KCNJ2* (Potassium Voltage-Gated Channel Subfamily J Member 2) (65,113). Pacemaker cells are traditionally known for lacking Kir2.1 channels, and thus displaying no I_{K1} , besides expressing the HCN4 channel, which produces the depolarizing pacemaker I_f current (113,124).

The persistence of spontaneous AP firing could be due to a low expression of Kir2.1 (not assessed by us). In fact, Kir 2.1 expression has hardly been detected in *in vitro* differentiated cardiomyocytes throughout the literature, being often held accountable for the rather unstable RMP of hPSC-CM (110,113,117). In addition to this, a persistent expression of the HCN4 channel and of the I_f has largely been reported in hPSC-CM, and could possibly explain the high automaticity observed in these cells (37).

The average RMP observed in this study are consistently more hyperpolarized than -77mV, with many observations averaging around -85mV (Fig.9d). This is an interesting achievement, considering that although the native cardiac RMP is -85mV (41), most ventricular-like hiPSC-CM in the literature display way more depolarized RMP, ranging from 68mV to -50mV (115,117,121,122,125). In spite of their more hyperpolarized RMP, the AP

amplitudes of the hiPSC-CM analysed in this study (Fig.9c) still fall short of that seen in native APs ($>100\text{mV}$) (2), being coherent with what was verified by other authors (24,103).

Zhao and collaborators (119) analysed the kinetic properties of APs on day 30 and 60 of differentiation and reported no significant variation on RMP, APA, dV/dT_{max} , or $\text{APD}_{50/90}$. They also confirmed the activity of ion currents that mostly contribute to the cardiac AP. Most ion currents tested did not exhibit any time-dependent significant changes. On the other hand, Sheng (118) report no changes in RPM, but an increased dV/dT_{max} and a generally reduced $\text{APD}_{50/90}$ on day 60 compared to day 20. Such increase in depolarization velocity can be explained by the time-dependent increase in Na^+ currents observed in that study. Because a $\sim 100\%$ average increase in total L-type Ca^{2+} currents on day 60 in comparison to day 20 was observed on this work, this cannot explain the general decrease on AP duration of these cells. Our results reveal only a tendency to increase dV/dT_{max} (Fig.9b) in older hiPSC-CM, but an analysis of each ion current that could confirm or refute this observed tendency has not been performed. The magnitude of dV/dT_{max} found in the present study is smaller than that reported by a series of studies which observe upstroke velocities ranging from 11-15V/s on hiPSC-CM (42,117,118,121), but is in line with that reported by BurrIDGE (2015) (122).

In summary, we have characterized APs from hiPSC-CM in different timepoints and verified that these cells fire APs spontaneously and possess kinetic properties which are compatible with others verified in the literature (42,117,118,121,122,125) and which do not significantly vary with time.

7.3 Effect of modulation of B2R on the molecular maturation of hiPSC-CM

Although the liver is the greatest site of kininogen and kallikrein synthesis, HMWK, LMWK and prekallikrein have been identified in other sites of the human body, such as the kidney, brain, pancreas, lungs and heart (127). In addition to this, it is known that the B2R is

constitutively expressed outside the cardiovascular system as well (74,128), which likely means it exerts other physiological functions in other tissues of the body beyond the control of vasodilation.

Indeed, bradykinin control of blood pressure through eicosanoids and nitric oxide-mediated vasodilation has been long described over the last decades (81,129–131). Further evidences suggest that BK acts not only on endothelial cells but also on the heart itself. For instance, high affinity B2 receptors have been reported in rat cardiomyocytes and cardiac fibroblasts (132). Examples of BK action on the heart are its protective effect over the development of left ventricular hypertrophy, myocardial ischemia and heart remodelling following infarction (129,132–134).

Our group has studied, over the years, the mechanisms through which KKS (kinin-kallikrein system and its receptors) modulates key cellular processes in neurons, such as cell proliferation (83) and differentiation (74,76,77,79,135). Moreover, additional unpublished data from our group (80) and by others (102) suggests that BK aids skeletal muscle regeneration and differentiation. Considering these data and the preponderant effects that BK has on cardiovascular homeostasis, this study has sought understanding a possible impact of BK over the maturation of cardiomyocytes differentiated from hiPSC sources.

hiPSC are an ingenious technology which revolutionized medical research in the last decade. (136). It has been largely used to model genetic diseases and developmental processes, as well as in drug toxicity screenings (8,29). Ultimately, properly differentiated and mature hiPSC could be used in regenerative medicine.

Throughout the literature the onset of spontaneous contractions in hiPSC-CM has been reported to occur between the 5th and 10th day after hiPSC are induced to differentiate into cardiomyocytes (45,48). Using the differentiation protocol established by PluriCell Biotech,

cells consistently start contracting on the 5th or 6th day of differentiation (data not shown), and on the 5th day at least two thirds of the population already present a muscle phenotype, expressing cardiac sarcomeric proteins (Fig.6). Considering that the 5th day of differentiation seems like a key day for the commitment of differentiated cells with a cardiac muscle phenotype, preceding functional and molecular maturation, we chose this moment as the initial day to start stimulating or inhibiting the B2R (with BK or Firazyr, respectively).

In order to confirm that components of the KKS are expressed on hiPSC-CM employed in this study, total protein extracts were recovered from cardiomyocytes on the 5th day of differentiation. The qualitative analysis of the western blots (Fig.10) revealed the expression of the B2 receptor, meaning that the KKS signalling could be active at endogenous/basal levels in these cells.

Aiming to assess whether B2R was active on the cellular membrane, we performed a dose-response assays of BK stimulation of 5 days-old hiPSC-CM, using the technique of Ca^{2+} imaging (Fig.11). It was possible to confirm that the activation of B2R led to release of intracellular Ca^{2+} from sarcoplasmic stocks, probably through an IP3-mediated mechanism (as described in the introduction).

Although, for technical reasons, we have not performed the imaging of the cells following the pharmacological inhibition of the receptor, we have reasons to believe that the response is really coming from B2R stimulation and not from B1R: first, it is known that BK has an approximate 20.000-fold bigger affinity for B2R than for B1R (83). Second, B2R stimulation leads to transient Ca^{2+} release from intracellular stocks, regardless of extracellular Ca^{2+} availability. B1R, on the other hand, elicits a sustained release of intracellular Ca^{2+} but in a way that is dependent on Ca^{2+} influx from the extracellular environment (127). Considering that the Ca^{2+} imaging experiments were performed in a Ca^{2+} free buffer solution and that free

Ca^{2+} concentration returns to basal levels after only 60 seconds of stimulation (Fig.11a), we concluded that the observed response is very likely due to B2R stimulation.

We then decided to treat the cells with 10 μM BK from the 5th-15th day of differentiation (during 10 days of the maturation period, therefore) and analyse if the treatments had induced any change in the expression of molecular markers of maturation. Gene expression analysis of this material revealed no significant alterations on *TNNI1* nor *TNNI3* expression in relation to the control differentiation (Fig.11), and again, no changes were perceived on the protein expression of neither ssTnI, cTnI nor MLC2v (Fig.12).

The analysis of these results led us to question whether the treatment was really leading to the activation of pathways downstream of the B2R. In fact, a more careful look in the literature revealed that, unlike B1R, B2R can undergo phosphorylation upon repeated or prolonged receptor stimulation, resulting in receptor desensitization and disruption of downstream signalling pathways (127,137). Another mechanism of desensitization would be an association with invaginations of the plasma membrane, with transient receptor internalization (83).

In fact, the EC_{50} of bradykinin is 3nM on human umbilical veins (138) and 12nM in human fibroblasts (139), which means that the employed dose of 10 μM is approximately 1000-thousand fold bigger than the receptor EC_{50} . Based on this, and on the fact that the dose of 1 μM BK has been shown to improve neuronal differentiation (74,77,79), we decided to test the effect of a 1 μM BK on hiPSC-CM maturation.

After a 25-day long treatment with either 1 μM BK or 5 μM Firazyr + 1 μM BK it was not possible to discern any significant effect of B2R modulation on the gene and protein expression levels of skeletal and cardiac troponin I (Fig.14). Although unlikely, it could be possible that a ratiometric technique like western blot could reveal variations in the net

quantities of total cTnI or ssTnI expression, as this cannot be verified by the flow cytometry technique. Finally, the proportion of ventricular cells in the differentiated population seems to remain stable following B2R activation or inhibition.

However, the possibility that B2R modulation exerts other effects which have not been assessed in the study cannot be ruled out. We suggest that screening experiments be used to verify which intracellular signalling pathways become active in response to BK stimulation. For instance, activation of MAPK/ERK pathway has been reported following BK modulation of neuronal differentiation (79). Further results from our group show Akt phosphorylation upon BK stimulation, suggesting activation of the PI3K-Akt pathway (135). Moreover, a 10nM dose of BK has been reported to regulate cell cycle progression and migration in cardiac precursors through activation of both MAPK/ERK and PI3K-Akt pathways (103). Based on this, we could hypothesise that modulation of B2R activity could have effects on hiPSC-CM proliferation, which has not been assessed by us. Alternatively, it could be that, on cardiomyocytes, 1 μ M BK still leads to receptor desensitization, hampering its effects over cardiomyogenic differentiation and maturation.

More information about which signalling pathways transduce bradykinin's effects on hiPSC-CM could, ultimately, allow more insights about what cellular processes should be further investigated.

CONCLUSIONS

8. CONCLUSIONS

We have observed a significant effect of culture time on the maturation of hiPSC-CM regarding the expression of *TNNI1* and *TNNI3* genes, with an increasing prevalence of *TNNI3* expression of *TNNI1*. Such observations could not be fully confirmed from the analysis of the protein levels of the troponin isoforms, although this could reflect a limitation of the technique employed. Still, we conclude that the shift in troponin I expression is a reasonable maturation marker in the employed model.

In addition to this, we have also verified a consistent time-dependent increase in the ventricular phenotype as differentiation and maturation progress, owing to the increase in the frequency of ventricular-like APs, as well as of the expression of the ventricular marker MLC2v.

The electrophysiological properties of the cells are coherent with that reported by other studies that differentiate cardiomyocytes from PSCs, showing APs morphologies that are overall similar to native APs, but that still fall behind regarding automaticity and some kinetic parameters such as depolarization velocity and amplitude.

Regarding the effect of B2R activation or inhibition in hiPSC-CM, we could perceive no clear effect of BK or Firazyr on the expression of maturation markers, nor any shift on the expression of the subtype marker MLC2v. It appears that the KKS is not acting on the *in vitro* maturation of hiPSC-CM, nor on the specification of subtype fate. We do not discard the possibility that BK could be leading to other unexplored effects and recommend a closer look at which intracellular signalling pathways become active following BK stimulation, in order to narrow down, which cellular processes should be further investigated.

BIBLIOGRAPHIC REFERENCES

9. BIBLIOGRAPHIC REFERENCES

1. Mendis S, Puska P, Norrving B. Global atlas on cardiovascular disease prevention and control. World Heal Organ. 2011;2–14.
2. Sigg, Daniel C.; Laizzo, Paul A.; Xiao, Yong-Fu; He B. Cardiac Electrophysiology Methods and Models. Cardiac Electrophysiology Methods and Models. 2010. 41-349 p.
3. Milan DJ, MacRae CA. Animal models for arrhythmias. Cardiovasc Res. 2005;67(3):426–37.
4. Ma R, Liang J, Huang W, Guo L, Cai W, Wang L, et al. Electrical Stimulation Enhances Cardiac Differentiation of Human Induced Pluripotent Stem Cells for Myocardial Infarction Therapy. Antioxid Redox Signal. 2017;6:1–53.
5. Nigro P, Bassetti B, Cavallotti L, Catto V, Carbucicchio C, Pompilio G. Cell therapy for heart disease after 15 years: Unmet expectations. Pharmacol Res. 2018;127:77–91.
6. Funakoshi S, Miki K, Takaki T, Okubo C, Hatani T, Chonabayashi K, et al. Enhanced engraftment, proliferation, and therapeutic potential in heart using optimized human iPSC-derived cardiomyocytes. Sci Rep. 2016;6(January):1–14.
7. Chan AT, Karakas MF, Vakrou S, Afzal J, Rittenbach A, Lin X, et al. Hyaluronic Acid-Serum Hydrogels Rapidly Restore Metabolism of Encapsulated Stem Cells and Promote Engraftment. Biomaterials. 2015 [cited 2017 May 20];73:1–11.
8. Sinnecker D, Laugwitz K-L, Moretti A. Induced pluripotent stem cell-derived cardiomyocytes for drug development and toxicity testing. Pharmacol Ther. 2014;143:246–52.
9. Zhou, Pingzhu; Pu WT. Recounting cardiac cellular composition. Circ Res. 2016;118(3):368–70.
10. Difrancesco D. The role of the funny current in pacemaker activity. Circ Res. 2010;106(3):434–46.
11. Hall, John E.; Guyton AC. Guyton and Hall textbook of medical physiology. In: 11th, editor. Guyton and Hall textbook of medical physiology. Elsevier; 2006.
12. Casimiro MC, Knollmann BC, Ebert SN, Vary JC, Greene a E, Franz MR, et al. Targeted disruption of the *Kcnq1* gene produces a mouse model of Jervell and Lange-Nielsen Syndrome. PNAS. 2001;98(5):2526–31.
13. Kim C, Wong J, Wen J, Wang S, Wang C, Spiering S, et al. Studying arrhythmogenic right ventricular dysplasia with patient-specific iPSCs. Nature. 2013;494(7435):105–10.
14. Lee MP, Ravenel JD, Hu RJ, Lustig LR, Tomaselli G, Berger RD, et al. Targeted disruption of the *Kvlqt1* gene causes deafness and gastric hyperplasia in mice. J Clin Invest. 2000;106(12):1447–55.
15. Brouillette J, Clark RB, Giles WR, Fiset C. Functional properties of K⁺ currents in adult mouse ventricular myocytes. J Physiol. 2004;559:777–98.
16. Marbán E. Cardiac channelopathies. Nature. 2002;415:213–8.
17. Sanguinetti MC, Tristani-Firouzi M. hERG potassium channels and cardiac arrhythmia. Nature. 2006;440(March):463–9.
18. Li RK, Tumati LC, Weisel RD, Mickle DAG. Isolation of cardiomyocytes from

- human myocardium for primary cell culturing. *J tissue Cult methods*. 1993;15:147–54.
19. Thomson J a, Itskovitz-eldor J, Shapiro SS, Waknitz M a, Swiergiel JJ, Marshall VS, et al. Embryonic Stem Cell Lines Derived from Human Blastocysts. *Science* (80-). 1998;282(November):1145–8.
 20. Kehat I, Kenyagin-Karsenti D. Human embryonic stem cells can differentiate into myocytes with structural and functional properties of cardiomyocytes. *J Clin Invest*. 2001;108(3):407–14.
 21. Mummery C. Differentiation of Human Embryonic Stem Cells to Cardiomyocytes: Role of Coculture With Visceral Endoderm-Like Cells. *Circulation*. 2003;107:2733–40.
 22. BurrIDGE PW, Anderson D, Priddle H, Barbadillo Muñoz MD, Chamberlain S, Allegrucci C, et al. Improved human embryonic stem cell embryoid body homogeneity and cardiomyocyte differentiation from a novel V-96 plate aggregation system highlights interline variability. *Stem Cells*. 2007;25(4):929–38.
 23. Takahashi K, Yamanaka S. Induction of pluripotent stem cells from mouse embryonic and adult fibroblast cultures by defined factors. *Cell*. 2006 Aug 25;126:663–76.
 24. Zhang J, Wilson GF, Soerens AG, Koonce CH, Yu J, Palecek SP, et al. Functional cardiomyocytes derived from human induced pluripotent stem cells. *Circ Res*. 2009;104(4).
 25. Tanaka T, Tohyama S, Murata M, Nomura F, Kaneko T, Chen H, et al. In vitro pharmacologic testing using human induced pluripotent stem cell-derived cardiomyocytes. *Biochem Biophys Res Commun*. 2009;385:497–502.
 26. Grimm FA, Iwata Y, Sirenko O, Bittner M, Rusyn I. High-Content Assay Multiplexing for Toxicity Screening in Induced Pluripotent Stem Cell-Derived Cardiomyocytes and Hepatocytes. *Assay Drug Dev Technol*. 2015;13(9):529–46.
 27. Itzhaki I, Maizels L, Huber I, Zwi-Dantsis L, Caspi O, Winterstern A, et al. Modelling the long QT syndrome with induced pluripotent stem cells. *Nature*. 2011;471:225–9.
 28. Heineke J, Molkentin JD. Regulation of cardiac hypertrophy by intracellular signalling pathways. *Nat Rev Mol Cell Biol*. 2006;7:589–600.
 29. Moretti A, Laugwitz K-L, Dorn T, Sinnecker D, Mummery C. Pluripotent Stem Cell Models of Human Heart Disease. *Cold Spring Harb Perspect Med*. 2013;3:1–20.
 30. Talkhabi M, Aghdami N, Baharvand H. Human cardiomyocyte generation from pluripotent stem cells: A state-of-art. *Life Sci*. 2016;145:98–113.
 31. Galdos FX, Guo Y, Paige SL, Vandusen NJ, Wu SM, Pu WT. Cardiac Regeneration: Lessons from Development. *Circ Res*. 2017;120(6):941–59.
 32. Kolanowski TJ, Antos CL, Guan K. Making human cardiomyocytes up to date: Derivation, maturation state and perspectives. *Int J Cardiol*. 2017;241:379–86.
 33. Small EM, Krieg PA. Molecular Regulation of Cardiac Chamber-Specific Gene Expression. *Trends Cardiovasc Med*. 2004;14(1):13–8.
 34. Piccini I, Rao J, Seebohm G, Greber B. Human pluripotent stem cell-derived cardiomyocytes: Genome-wide expression profiling of long-term in vitro maturation in comparison to human heart tissue. *Genomics Data*. 2015;4:69–72.
 35. Josowitz R, Lu J, Falce C, D’Souza SL, Wu M, Cohen N, et al. Identification and purification of human induced pluripotent stem cell-derived atrial-like cardiomyocytes

- based on sarcolipin expression. *PLoS One*. 2014;9(7):1–8.
36. Yanagi K, Takano M, Narazaki G, Uosaki H, Hoshino T, Ishii T, et al. Hyperpolarization-activated cyclic nucleotide-gated channels and T-type calcium channels confer automaticity of embryonic stem cell-derived cardiomyocytes. *Stem Cells*. 2007;25:2712–9.
 37. Kane C, Terracciano CMN. Concise Reviews: Criteria for Chamber-Specific Categorization of Human Cardiac Myocytes Derived from Pluripotent Stem Cells. *Stem Cells*. 2017;
 38. Yechikov S, Copaciu R, Gluck JM, Deng W, Chiamvimonvat N, Chan JW, et al. Same-Single-Cell Analysis of Pacemaker-Specific Markers in Human Induced Pluripotent Stem Cell-Derived Cardiomyocyte Subtypes Classified by Electrophysiology. *Stem Cells*. 2016;34(11):2670–80.
 39. Chen Z, Xian W, Bellin M, Dorn T, Tian Q, Goedel A, et al. Subtype-specific promoter-driven action potential imaging for precise disease modelling and drug testing in hiPSC-derived cardiomyocytes. *Eur Heart J*. 2016;38(4):1–10.
 40. Dunn, Kaitlin K.; Palecek SP. Engineering Scalable Manufacturing of High-Quality Stem Cell-Derived Cardiomyocytes for Cardiac Tissue Repair. *Front Med*. 2018;5:1–18.
 41. Liu J, Laksman Z, Backx PH. The electrophysiological development of cardiomyocytes. *Adv Drug Deliv Rev*. 2016;96:253–73.
 42. Barbuti A, Benzoni P, Campostrini G, Dell’Era P. Human derived cardiomyocytes: A decade of knowledge after the discovery of induced pluripotent stem cells. *Dev Dyn* 2016 Dec;245:1145–58.
 43. Wang, Y; Xu, Huaying, Kumar, Rajiv, Tipparaju, Srinivas, M.; Wagner, Mary B.; Joyner RW. Differences in transient outward current properties between neonatal and adult human atrial myocytes. *J Mol Cell Cardiol*. 2003;35:1083–92.
 44. Karakikes I, Senyei GD, Hansen J, Kong C-W, Azeloglu EU, Stillitano F, et al. Small molecule-mediated directed differentiation of human embryonic stem cells toward ventricular cardiomyocytes. *Stem Cells Transl Med*. 2014;3(1):18–31.
 45. Weng Z, Kong C-W, Ren L, Karakikes I, Geng L, He J, et al. A Simple, Cost-Effective but Highly Efficient System for Deriving Ventricular Cardiomyocytes from Human Pluripotent Stem Cells. *Stem Cells Dev*. 2014;23(14):1704–16.
 46. Zhang Q, Jiang J, Han P, Yuan Q, Zhang J, Zhang X, et al. Direct differentiation of atrial and ventricular myocytes from human embryonic stem cells by alternating retinoid signals. *Cell Res*. 2011;21:579–87.
 47. Ou D-B, Lang H-J, Chen R, Liu X-T, Zheng Q-S. Using embryonic stem cells to form a biological pacemaker via tissue engineering technology. *BioEssays*. 2009;31:246–52.
 48. Schweizer PA, Darche FF, Ullrich ND, Geschwill P, Greber B, Rivinius R, et al. Subtype-specific differentiation of cardiac pacemaker cell clusters from human induced pluripotent stem cells. *Stem Cell Res Ther*. 2017;8(8):1–15.
 49. Kleger A, Seufferlein T, Malan D, Tischendorf M, Storch A, Wolheim A, et al. Modulation of calcium-activated potassium channels induces cardiogenesis of pluripotent stem cells and enrichment of pacemaker-like cells. *Circulation*. 2010;122(18):1823–36.
 50. Xu XQ, Soo SY, Sun W, Zweigerdt R. Global expression profile of highly enriched

- cardiomyocytes derived from human embryonic stem cells. *Stem Cells*. 2009;27:2163–74.
51. Yang X, Pabon L, Murry CE. Engineering adolescence: Maturation of human pluripotent stem cell-derived cardiomyocytes. *Circ Res*. 2014;114(3):511–23.
 52. Solaro RJ. Sarcomere control mechanisms and the dynamics of the cardiac cycle. *J Biomed Biotechnol*. 2010;2010:1–10.
 53. Sheng, Juan-Juan; Jin J-P. TNNI1, TNNI2 and TNNI3: Evolution, Regulation and Protein Structure-Function Relationships. *Gene*. 2016;576:385–94.
 54. Bedada FB, Wheelwright M, Metzger JM. Maturation status of sarcomere structure and function in human iPSC-derived cardiac myocytes. *Biochim Biophys Acta*. 2015;1863(7):1829–38.
 55. Burggreen, Warren W.; Keller BB. Development of Cardiovascular Systems - Molecules to Organisms. Burggren, Warren W.; Keller BB, editor. Cambridge: Cambridge University Press; 1997. 27-34 p.
 56. Katrukha IA. Human cardiac troponin complex. Structure and functions. *Biochemistry*. 2013;78(13):1447–65.
 57. Bedada FB, Chan SSK, Metzger SK, Zhang L, Zhang J, Garry DJ, et al. Acquisition of a quantitative, stoichiometrically conserved ratiometric marker of maturation status in stem cell-derived cardiac myocytes. *Stem Cell Reports* . 2014;3(4):594–605.
 58. Rao C, Prodromakis T, Kolker L, Chaudhry U a R, Trantidou T, Sridhar A, et al. The effect of microgrooved culture substrates on calcium cycling of cardiac myocytes derived from human induced pluripotent stem cells. *Biomaterials*. 2013;34:2399–411.
 59. Zhang GQ, Wei H, Lu J, Wong P, Shim W. Identification and Characterization of Calcium Sparks in Cardiomyocytes Derived from Human Induced Pluripotent Stem Cells. *PLoS One*. 2013;8(2):1–11.
 60. Satin J, Itzhaki I, Rapoport S, Schroder E a, Izu L, Arbel G, et al. Calcium handling in human embryonic stem cell-derived cardiomyocytes. *Stem Cells*. 2008;26:1961–72.
 61. Itzhaki I, Schiller J, Beyar R, Satin J, Gepstein L. Calcium handling in embryonic stem cell-derived cardiac myocytes: Of mice and men. *Ann N Y Acad Sci*. 2006;1080:207–15.
 62. Yee-Ki, Lee; Chung-Wah S. Calcium handling in hiPSC-derived cardiomyocytes. *SpringerBriefs in Stem Cells*. Springer-Verlag New York; 2012. 1-47 p.
 63. Hasenfuss G, Mulieri LA, Blanchard EM, Holubarsch C, Leavitt BJ, Ittleman F, et al. Energetics of isometric force development in control and volume- overload human myocardium. Comparison with animal species. *Circ Res*. 1991;68:836–46.
 64. Ben-Ari M, Naor S, Zeevi-Levin N, Schick R, Jehuda R Ben, Reiter I, et al. Developmental changes in electrophysiological characteristics of human induced Pluripotent Stem Cell-derived cardiomyocytes. *Hear Rhythm Soc*. 2016;13(12):2379–87.
 65. Sartiani L, Bettiol E, Stillitano F, Mugelli A, Cerbai E, Jaconi ME. Developmental changes in cardiomyocytes differentiated from human embryonic stem cells: a molecular and electrophysiological approach. *Stem Cells*. 2007;25:1136–44.
 66. Lundy SD, Zhu W-Z, Regnier M, Laflamme MA. Structural and functional maturation of cardiomyocytes derived from human pluripotent stem cells. *Stem Cells Dev*.

- 2013;22(14):1991–2002.
67. Chun YW, Balikov D a, Feaster TK, Williams CH, Sheng CC, Lee J-B, et al. Combinatorial polymer matrices enhance in vitro maturation of human induced pluripotent stem cell-derived cardiomyocytes. *Biomaterials*. 2015;67:52–64.
 68. Zhou H, Dickson ME, Kim MS, Bassel-Duby R, Olson EN. Akt1/protein kinase B enhances transcriptional reprogramming of fibroblasts to functional cardiomyocytes. *Proc Natl Acad Sci*. 2015;112(38):11864–9.
 69. Wang D, Chao L, Chao J. Hypotension in Transgenic Mice Overexpressing Human Bradykinin B2 receptor. *Hypertension*. 1997;29(1):488–93.
 70. Tsai Y-J, Hao S-P, Chen C-L, Lin BJ, Wu W-B. Involvement of b2 receptor in bradykinin-induced proliferation and proinflammatory effects in human nasal mucosa-derived fibroblasts isolated from chronic rhinosinusitis patients. *PLoS One*. 2015;10(5):1–19.
 71. Tschöpe C, Westermann D. Development of diabetic cardiomyopathy and the kallikrein-kinin system - New insights from B1 and B2 receptor signaling. *Biol Chem*. 2008;389(6):707–11.
 72. Dendorfer a, Wolfrum S, Dominiak P. Pharmacology and cardiovascular implications of the kinin-kallikrein system. Vol. 79, *Japanese journal of pharmacology*. 1999. p. 403–26.
 73. Murugesan P, Hildebrandt T, Bernlöhner C, Lee D, Khang G, Doods H, et al. Inhibition of Kinin B1 Receptors Attenuates Pulmonary Hypertension and Vascular Remodeling Novelty and Significance.
 74. Martins AHB, Resende RR, Majumder P, Faria M, Casarini DE, Ta A, et al. Neuronal Differentiation of P19 Embryonal Carcinoma Cells Modulates Kinin B2 Receptor Gene Expression and Function *. *J Biol Chem*. 2005;280(20):19576–86.
 75. Martins a H, Alves JM, Trujillo C a, Schwindt TT, Barnabe GF, Motta FL, et al. Kinin-B2 receptor expression and activity during differentiation of embryonic rat neurospheres. *Cytom A*. 2008;73:361–8.
 76. Trujillo C a., Schwindt TT, Martins AH, Alves JM, Mello LE, Ulrich H. Novel perspectives of neural stem cell differentiation: From neurotransmitters to therapeutics. *Cytom Part A*. 2009;75(A):38–53.
 77. Nascimento IC, Glaser T, Nery A a., Pillat MM, Pesquero JB, Ulrich H. Kinin-B1 and B2 receptor activity in proliferation and neural phenotype determination of mouse embryonic stem cells. *Cytom Part A*. 2015;87(11):989–1000.
 78. Huang, Zhenhua ; Yu, Jun; Toselli, Paul; Bhawan, Jag; Sudireddy, Vasanthi; Taylor, Linda; Polgar P. Angiotensin II Type 1 and Bradykinin B2 receptors expressed in early stage epithelial cells derived from human embryonic stem cells. *J Cell Physiol*. 2007;211(1):816–25.
 79. Pillat MM, Lameu C, Trujillo CA, Glaser T, Cappellari AR, Negraes PD, et al. Bradykinin promotes neuron-generating division of neural progenitor cells through ERK activation. *Co Biol*. 2016;129:3437–48.
 80. Alves JM, Martins AH, Lameu C, Glaser T, Boukli NM, Bassaneze V, et al. Kinin-B2 receptor activity in skeletal muscle regeneration and myoblast differentiation. :1–12.
 81. Abelous J.; Bardier E. Les substances hypotensives de l'urine humaine normale. *Compt Rend Soc Biol*. 1909;(66):511–2.

82. Jacobsen S. Separation of two different substrates for plasma kinin-forming enzymes. *Nature*. 1966;210:98–9.
83. Leeb-Lundberg FL., Marceau F, Müller-esterl W, Pettibone DJ, Zuraw BL. International Union of Pharmacology. XLV. Classification of the Kinin Receptor Family: from Molecular Mechanisms to Pathophysiological Consequences. *Pharmacol Rev*. 2005;57(1):27–77.
84. Bhoola, K D; Figueroa, C.D.; Worthy K. Bioregulation of Kinins : kallikreins, kininogens and kininases. *Pharmacological Rev*. 1992;44(1):1–80.
85. Cyr M, Lepage Y, Blais C, Gervais N, Cugno M, Rouleau JL, et al. Bradykinin and des-Arg(9)-bradykinin metabolic pathways and kinetics of activation of human plasma. *Am J Physiol Heart Circ Physiol*. 2001;281(1):H275–83.
86. Moraes MS, Costa PE, Batista WL, Paschoalin T, Curcio MF, Borges RE, et al. Endothelium-derived nitric oxide (NO) activates the NO-epidermal growth factor receptor-mediated signaling pathway in bradykinin-stimulated angiogenesis. *Arch Biochem Biophys*. 2014;558:14–27.
87. Yayama K, Nagaoka M, Takano M, Okamoto H. Expression of kininogen, kallikrein and kinin receptor genes by rat cardiomyocytes. *Biochim Biophys Acta*. 2000;1495:69–77.
88. Newton AC. Protein kinase C: perfectly balanced. *Crit Rev Biochem Mol Biol*. 2018;53(2):208–30.
89. Freay a., Johns A, Adams DJ, Ryan US, Van Breemen C. Bradykinin and inositol 1,4,5-trisphosphate-stimulated calcium release from intracellular stores in cultured bovine endothelial cells. *Pfluegers Arch Eur J Physiol*. 1989;414:377–84.
90. Schlossmann J, Ammendola A, Ashman K, Zong X, Huber A, Neubauer G, et al. Regulation of intracellular calcium by a signalling complex of IRAG, IP3 receptor and cGMP kinase I β . *Nature*. 2000;404:197–201.
91. Golias C, Charalabopoulos A, Stagikas D, Charalabopoulos K, Batistatou A. The kinin system - bradykinin: biological effects and clinical implications. Multiple role of the kinin system - bradykinin. *Hippokratia*. 2007;11(3):124–8.
92. Corbit KC, Trakul N, Eves EM, Diaz B, Marshall M, Rosner MR. Activation of Raf-1 signaling by protein kinase C through a mechanism involving Raf kinase inhibitory protein. *J Biol Chem*. 2003;278(15):13061–8.
93. Hunter, Tony; Ling, Nicholas; Cooper JA. Protein kinase C phosphorylation of the EGF receptor at a threonine residue close to the cytoplasmic face of the plasma membrane. *Nature*. 1984;311:480–3.
94. Ueda Y, Hirai SI, Osada SI, Suzuki A, Mizuno K, Ohno S. Protein kinase C δ activates the MEK-ERK pathway in a manner independent of Ras and dependent on Raf. *J Biol Chem*. 1996;271(38):23512–9.
95. Madeddu P, Emanuelli C, Gaspa L, Salis B, Milia AF, Chao L, et al. Role of the bradykinin B2 receptor in the maturation of blood pressure phenotype: Lesson from transgenic and knockout mice. *Immunopharmacology*. 1999;44:9–13.
96. Bouhadjane M, Kaszas A, Raszsa B, Harris-Warrick RM, Vinay L, Brocard F. Sensitization of neonatal rat lumbar motoneuron by the inflammatory pain mediator bradykinin. *Elife*. 2015;4:1–23.
97. Campbell DJ. Towards understanding the kallikrein-kinin system: Insights from

- measurement of kinin peptides. *Brazilian J Med Biol Res.* 2000;33(6):665–7.
98. Roman-Campos D, Duarte HL, Gomes ER, Castro CH, Guatimosim S, Natali AJ, et al. Investigation of the cardiomyocyte dysfunction in bradykinin type 2 receptor knockout mice. *Life Sci.* 2010;87:715–23.
 99. Trabold F, Pons S, Hagege A a., Bloch-Faure M, Alhenc-Gelas F, Giudicelli JF, et al. Cardiovascular phenotypes of kinin B2 receptor- and tissue kallikrein-deficient mice. *Hypertension.* 2002;40(1):90–5.
 100. Goldstein RH, Wall M. Activation of protein formation and cell division by bradykinin and des-Arg9-bradykinin. *J Biol Chem.* 1984;259(14):9263–8.
 101. Sheng Z, Yao Y, Li Y, Yan F, Huang J, Ma G. Bradykinin preconditioning improves therapeutic potential of human endothelial progenitor cells in infarcted myocardium. *PLoS One.* 2013;8(12):1–13.
 102. Bruno G, Cencetti F, Bernacchioni C, Donati C, Blankenbach KV, Thomas D, et al. Bradykinin mediates myogenic differentiation in murine myoblasts through the involvement of SK1/Spns2/S1P2axis. *Cell Signal.* 2018;45:110–21.
 103. Li G, Wang Y, Li G-R. Bradykinin regulates cell growth and migration in cultured human cardiac c-Kit⁺ progenitor cells. *Oncotarget.* 2017;8(7):10822–35.
 104. Wei W, Huang W, Yue J. Requirement of IP3 receptor 3 (IP3R3) in nitric oxide induced cardiomyocyte differentiation of mouse embryonic stem cells. *Exp Cell Res.* 2016;346:9–16.
 105. Bae SW, Kim HS, Cha YN, Park YS, Jo SA, Jo I. Rapid increase in endothelial nitric oxide production by bradykinin is mediated by protein kinase A signaling pathway. *Biochem Biophys Res Commun.* 2003;306:981–7.
 106. Sakamoto N, Uemura H, Hara Y, Saito T, Masuda Y, Nakaya H. Bradykinin B2-receptor-mediated modulation of membrane currents in guinea-pig cardiomyocytes. *Br J Pharmacol.* 1998;125:283–92.
 107. DeLaughter DM, Bick AG, Wakimoto H, McKean D, Gorham JM, Kathiriyi IS, et al. Single-Cell Resolution of Temporal Gene Expression during Heart Development. *Dev Cell.* 2016;39(4):480–90.
 108. Xu C, Wang L, Yu Y, Yin F, Zhang X, Jiang L, et al. Bioinspired onion epithelium-like structure promotes the maturation of cardiomyocytes derived from human pluripotent stem cells. *Biomater Sci.* 2017;29:4–16.
 109. Jeziorowska D, Fontaine V, Jouve C, Villard E, Dussaud S, Akbar D, et al. Differential sarcomere and electrophysiological maturation of human iPSC-derived cardiac myocytes in monolayer vs. Aggregation-based differentiation protocols. *Int J Mol Sci.* 2017;18:1–16.
 110. Blazeski A, Tung L. Electrophysiological and contractile function of cardiomyocytes derived from human embryonic stem cells. *Prog Biophys Mol Biol.* 2012;110:178–95.
 111. Kadota S, Pabon L, Reinecke H, Murry CE. In Vivo Maturation of Human Induced Pluripotent Stem Cell-Derived Cardiomyocytes in Neonatal and Adult Rat Hearts. *Stem Cell Reports.* 2017;8:278–89.
 112. Peinkofer G, Burkert K, Krausgrill B, Urban K, Saric T, Hescheler J, et al. From early embryonic to adult stage: Comparative study of action potentials of native and pluripotent stem cell-derived cardiomyocytes. *Stem Cells Dev.* 2016;25(19):1397–406.

113. Van Den Heuvel NHL, Van Veen TAB, Lim B, Jonsson MKB. Lessons from the heart: Mirroring electrophysiological characteristics during cardiac development to in vitro differentiation of stem cell derived cardiomyocytes. *J Mol Cell Cardiol.* 2014;67:12–25.
114. Jeck CD, Boyden PA. Age-related appearance of outward currents may contribute to developmental differences in ventricular repolarization. *Circ Res.* 1992;71(6):1390–403.
115. Obreztschikova MN, Sosunov EA, Plotnikov A, Anyukhovskiy EP, Gainullin RZ, Danilo P, et al. Developmental changes in IKr and IKs contribute to age-related expression of dofetilide effects on repolarization and proarrhythmia. *Cardiovasc Res.* 2003;59(2):339–50.
116. Zhu R, Millrod MA, Zambidis ET, Tung L. Variability of Action Potentials Within and among Cardiac Cell Clusters Derived from Human Embryonic Stem Cells. *Sci Rep.* 2016;6:1–12.
117. Kim HS, Yoon JW, Li H, Jeong GO, Park JJ, Shin SE, et al. Functional expression and pharmaceutical efficacy of cardiac-specific ion channels in human embryonic stem cell-derived cardiomyocytes. *Sci Rep .* 2017;7(1):1–11.
118. Sheng X, Reppel M, Nguemo F, Mohammad FI, Kuzmenkin A, Hescheler J, et al. Human Pluripotent Stem Cell-Derived Cardiomyocytes: Response to TTX and Lidocaine Reveals Strong Cell to Cell Variability. *PLoS One.* 2012;7(9):1–12.
119. Zhao Z, Lan H, El-battrawy I, Li X, Buljubasic F, Sattler K, et al. Ion Channel Expression and Characterization in Human Induced Pluripotent Stem Cell-Derived Cardiomyocytes. *Stem Cells Int.* 2018;2018:1–14.
120. Otsuji TG, Minami I, Kurose Y, Yamauchi K, Tada M, Nakatsuji N. Progressive maturation in contracting cardiomyocytes derived from human embryonic stem cells: Qualitative effects on electrophysiological responses to drugs. *Stem Cell Res.* 2010;4:201–13.
121. He J-Q, Ma Y, Lee Y, Thomson JA, Kamp TJ. Human Embryonic Stem Cells Develop Into Multiple Types of Cardiac Myocytes: Action Potential Characterization. *Circ Res.* 2003;93:32–9.
122. Burridge PW et al. Chemically defined and small molecule-based generation of human cardiomyocytes. *Nat Methods.* 2014;11(8):855–60.
123. Robertson C, Tran D, George S. Concise Review: Maturation Phases of Human Pluripotent Stem Cell-Derived Cardiomyocytes. *Stem Cells .* 2013;31(5):1–17.
124. Matsuura H, Ehara T, Ding WG, Omatsu-Kanbe M, Isono T. Rapidly and slowly activating components of delayed rectifier K⁺ current in guinea-pig sino-atrial node pacemaker cells. *J Physiol.* 2002;540(3):815–30.
125. Lee S, Lee H-A, Choi SW, Kim SJ, Kim K-S. Evaluation of nefazodone-induced cardiotoxicity in human induced pluripotent stem cell-derived cardiomyocytes. *Toxicol Appl Pharmacol .* 2016;296:42–53.
126. Honda M, Kiyokawa J, Tabo M, Inoue T. Electrophysiological Characterization of Cardiomyocytes Derived From Human Induced Pluripotent Stem Cells. *J Pharmacol Sci.* 2011;117:149–59.
127. Campbell DJ. Bradykinin Peptides. In: *Handbook of Biologically Active Peptides .* Second Edi. Elsevier Inc.; 2013. p. 1386–93.

128. Regoli D, Plante GE, Gobeil F. Impact of kinins in the treatment of cardiovascular diseases. *Pharmacol Ther* . 2012;135(1):94–111.
129. Rhaleb NE, Yang XP, Carretero OA. The Kallikrein-Kinin system as a regulator of cardiovascular and renal function. *Compr Physiol*. 2011;1(2):971–93.
130. Kaplan AP. The bradykinin-forming cascade: A historical perspective. *Chem Immunol Allergy*. 2014;100:205–13.
131. Rocha e Silva M, Beraldo WT, Rosenfeld G. Bradykinin, a Hypotensive and Smooth Muscle Stimulating Factor Released From Plasma Globulin By Snake Venoms and By Trypsin. *Am J Physiol* . 1949;156(2):261–73.
132. Schölkens BA. Kinins in the cardiovascular system. *Immunopharmacology*. 1996;33:209–16.
133. Sharma JN. Cardiovascular activities of the bradykinin system. *Sci World J*. 2008;8:384–93.
134. Dell'Italia LJ, Oparil S. Bradykinin in the heart: Friend or foe? *Circulation*. 1999;100(23):2305–7.
135. Martins AH, Alves JM, Perez D, Carrasco M, Torres-Rivera W, Eterović VA, et al. Kinin-B2 receptor mediated neuroprotection after NMDA excitotoxicity is reversed in the presence of kinin-B1 receptor agonists. *PLoS One*. 2012;7(2):1–6.
136. Diecke S, Diecke S, Diecke S, Jung SM, Lee J, Lee J, et al. Recent technological updates and clinical applications of induced pluripotent stem cells. *Korean J Intern Med*. 2014;29(5):547–57.
137. Marceau F, Bachvarov DR. Kinin receptors. *Clin Rev Allergy Immunol*. 1998;16:385–401.
138. Bélanger S, Bovenzi V, Côté J, Neugebauer W, Amblard M, Martinez J, et al. Structure-activity relationships of novel peptide agonists of the human bradykinin B2 receptor. *Peptides*. 2009;30:777–87.
139. Mcallister B. S, Leeb-Lundberg FL., Javors MA, Olson MS. Bradykinin Receptors and Signal Transduction Pathways in Human Fibroblasts: Integral Role for Extracellular Calcium. *Arch Biochem Biophys* . 1993;304(1):294–301.

10. ANEXOS

A – SÚMULA CURRICULAR

1. DADOS PESSOAIS

Nome: Maria Elisa Almeida Góes

Local e Data de Nascimento: Rio de Janeiro, 27/02/1992

2. EDUCAÇÃO

Escola Internacional de Alphaville, Barueri, 2009

Universidade de São Paulo, São Paulo, 2015: Graduação em Ciências Biológicas

Universidade de São Paulo, São Paulo, 2018: Mestrado em Ciências Biológicas
(Bioquímica)

3. FORMAÇÃO COMPLEMENTAR

Intercâmbio de Graduação: Biomedical Sciences, Newcastle University, Newcastle Upon
Tyne (UK), 2013

4. OCUPAÇÃO

Bolsista de Mestrado: CNPq, 04/2016 – 04/2018

5. PUBLICAÇÕES